Metabarcoding supports regional ocean acidification monitoring and identifies novel bioindicators in the Southern California Bight

Ashton Bandy[1,2*], Christina A. Frieder[2*], Susanna Theroux[2], Zachary Gold[3], Sean M. McAllister[3,4], Katherine Mackey[1], Karen McLaughlin[2], Nataly Pineda[1], Melissa Brock[5], Martha Sutula[2], Adam Martiny[1,5]

1 Department of Earth System Science, University of California-Irvine, USA
2 Southern California Coastal Water Research Project, Costa Mesa, California, USA
3 Pacific Marine Environmental Laboratory, National Oceanic and Atmospheric Administration, Seattle, Washington, USA
4 Cooperative Institute for Climate, Ocean, and Ecosystem Studies, Seattle, Washington, USA
5 Department of Ecology and Evolutionary Biology, University of California-Irvine, USA

*abandy@uci.edu *christinaf@sccwrp.org

Abstract

The impacts of ocean acidification (OA) on marine communities are a growing concern for coastal upwelling ecosystems, such as the Southern California Bight (Bight). Successful management of coastal resources in the face of OA requires accurate assessment tools to understand the status and trends of OA impacts on biological communities. Current methods often rely on the condition of individual organisms (e.g., shell dissolution) and are resource- and labor-intensive. As a result, they are difficult to scale to population-level effects or to impacts on the community as a whole, which limits impact assessments and hinders implementation by coastal resource managers. DNA-based monitoring methods can address these gaps, and represent a scalable and cost-effective complement to traditional OA biomonitoring efforts. We applied a DNA metabarcoding approach to analyze mesozooplankton (>200 µm) samples in the Bight to investigate novel OA biomonitoring approaches and target organisms. We sequenced the mitochondrial cytochrome c oxidase subunit 1 (CO1) gene and analyzed mesozooplankton community composition across 20 locations and four seasons. We found communities largely structured by seasonal gradients and dominated by copepods and krill. A subset of taxa corresponded strongly to carbonate chemistry variability; taxa in the Order Cheilostomatida (encrusting bryozoans), along with the copepod species *Clausocalanus furcatus* and *Oncaea scottodicarloi* corresponded to high aragonite saturation state values. In contrast, other species like *Calanus pacificus* (calanoid copepod) and *Euphausia pacifica* (krill) corresponded with low aragonite saturation state. We also investigated the ubiquity and relative abundance of routine target organisms (pteropods and larval crabs) versus alternative targets. Pteropods were rare and only found in the wintertime, while other larval stages of benthic calcifiers were more relatively abundant and ubiquitous. Our findings highlight the utility of DNA-based methods to guide OA biomonitoring and lay the groundwork for future research on OA indicators in this region.

Introduction

The ocean absorbs roughly a quarter of human CO_2 emissions, leading to decreased seawater pH and altered carbonate chemistry, a process known as ocean acidification (OA) [1]. By lowering the survival, growth, and reproductive success of organisms, OA undermines populations and, over time, drives habitat loss and changes in community structure [2]. These changes are further compounded by multiple physiological stressors, including ocean hypoxia and warming, which are also accelerating with climate change [3–5].

Despite a wealth of research on the biological impacts of OA, scientific consensus on the best approaches to routinely monitor the status and trends of OA biological impacts is lacking. This presents a formidable challenge for scientists and managers looking to evaluate the biological impacts of OA or compare the magnitude of impacts across regions. Two general approaches are: 1) monitoring changes to general community structure and 2) targeted monitoring of specific organisms, typically either commercially-important or the most sensitive. Monitoring community structure is resource intensive and requires taxonomic expertise, which limits the scale and frequency at which this can be routinely employed. Targeted monitoring of calcifying zooplankton groups (such as pteropods, echinoderms, and decapods) either as population- or organism-level measures of fitness (e.g., shell dissolution) are strong candidates for biomonitoring of OA given their sensitivity to carbonate chemistry and ecological and commercial importance [6–8]. However, the suitability of these taxa depends on their spatiotemporal ubiquity, which is still unknown for many species of calcifying holoplankton and meroplankton [9, 10].

Rapid advancement of marine environmental DNA science in the past two decades can help address these fundamental knowledge gaps and implementation challenges across both community- and target organism-level approaches to monitoring. DNA metabarcoding approaches allow for the detection of organisms at trace levels, the differentiation of morphologically cryptic taxa, and the ability to survey multiple phylogenetic groups from a single sample, providing a depth of biological data that was previously unattainable [11]. This approach, particularly DNA metabarcode sequencing, has been successfully applied in research settings to evaluate marine biological responses to spatiotemporal environmental changes [12, 13], track zooplankton biodiversity in the Southern Ocean [14], assess Arctic marine biodiversity [15], and monitor food web connectivity along coastlines [16, 17], among many other applications. Metabarcoding has also been applied in the California Current System to evaluate marine vertebrate taxa [18] and delineate zooplankton biogeographic boundaries [19]. However, case studies of how to use DNA metabarcoding as a tool to support regional monitoring of OA biological impacts are still relatively scarce, particularly those that illustrate how such data can illuminate appropriate OA biological target organisms.

The Southern California Bight (i.e., the Bight) provides an opportunity to conduct such a case study for several reasons. First, this coastal ocean region is at the southern range of the California Current System (CCS), an upwelling-dominated eastern boundary ecosystem that has one of the highest rates of OA [20]. Seasonal, wind-driven upwelling brings deep waters with high dissolved inorganic carbon, low oxygen, and low pH to the surface, conditions further exacerbated by increasing anthropogenic carbon and potential climate-driven changes in upwelling intensity [21–23]. Although the Bight has so far experienced less extreme OA events compared to other CCS regions [24], its established vulnerability and the projected future increase in OA highlight the necessity for continuous monitoring to predict and mitigate the significant impacts on species [8]. Second, the Bight is home to several long-standing regional marine monitoring programs. The California Cooperative Oceanic Fisheries Investigations (CalCOFI) program has been monitoring zooplankton community structure in offshore regions of

the Bight and Central Coast via traditional taxonomy relative to gradients in ocean chemistry; only recently has this program began to evaluate the use of DNA metabarcoding [25]. In the nearshore Bight, the Southern California Bight Regional Monitoring Program (Bight RMP) has more recently been documenting the status and trends in carbonate chemistry and piloted coupled chemical and biological OA monitoring during their 2018 study [24]. Early work within the CCS identified assessment of shell dissolution via scanning electron micrograph as a leading OA-specific measure of biological stress [26]. Biological indicators have been most commonly examined with calcifying pteropods (e.g., *Limacina helicina*) and Dungeness crab megalopae (larval stage) as bioindicators that are the most sensitive to OA in the CCS [6, 7, 9, 27]. However, these microscopy-based methods are resource-intensive and only measure dissolution in the shells of a limited number of individuals [3, 6, 28]. In addition, the Bight lacks populations of Dungeness crab, so an analog species was chosen for the Bight RMP (*Emerita analoga*; Pacific Sand Crab), but it was not clear whether pteropods or *E. analoga* megalopae are the most suitable sentinel organisms for the Bight OA biomonitoring, or whether better alternatives exist.

For this reason, we undertook a pilot DNA metabarcoding study to investigate novel OA bioindicator assessments using both community trait-based and target organism approaches, as a complement to ongoing scanning electron micrograph analysis of shell dissolution in pteropods and *E. analoga* megalopae. In this study, we targeted mesozooplankton DNA using net tows collected across four seasons at 20 sites in the Bight to: (1) characterize diversity and composition, (2) assess correlations of carbonate-chemistry variables with trait-based taxonomic groupings and the overall mesozooplankton community to derive novel bioindicator candidates, and (3) evaluate the spatiotemporal ubiquity of current species-level targets (pteropods and *E. analoga*) compared to other meroplanktonic calcifiers that are frequently encountered in Bight RMP campaigns.

Methods

General overview

Field samples were collected during quarterly monitoring cruises as part of the Bight RMP. Twenty locations across the shelf of the Bight were sampled during four distinct seasons (Spring 2019, Summer 2019, Fall 2019, and Winter 2020), with each location sampled once per season for a total of 80 samples (Fig 1). Publicly Owned Treatment Works agencies (City of San Diego, City of Los Angeles, City of Oxnard, Orange County Sanitation District, and Los Angeles County Sanitation Districts) monitor these sites, which span the length of the coastal Bight, effectively capturing spatial variability within the region's dynamic oceanographic conditions. For more details including latitude/longitude for the sampling sites as well as sampling dates, see S1 Table.

Field sampling

Water-column profiles of temperature, salinity, dissolved oxygen, and pH were collected by CTD cast prior to each tow to a maximum depth of 150 m at most sites. Mesozooplankton were then sampled with double-ringed 200-µm bongo nets deployed from the stern using either an A-frame or crane, depending on vessel configuration. Oblique tows targeted approximately 150, 100, 50, and 25 m at 1.5-2 knots for $\sim$15, 10, 10, and 10 min, respectively ($\sim$45 min total). Tow depth was adjusted by wire scope to maintain a tow-line angle of about 45-60°, and a pressure sensor mounted on the tow yoke was used to verify depths achieved. Because the objective was to sample migrating

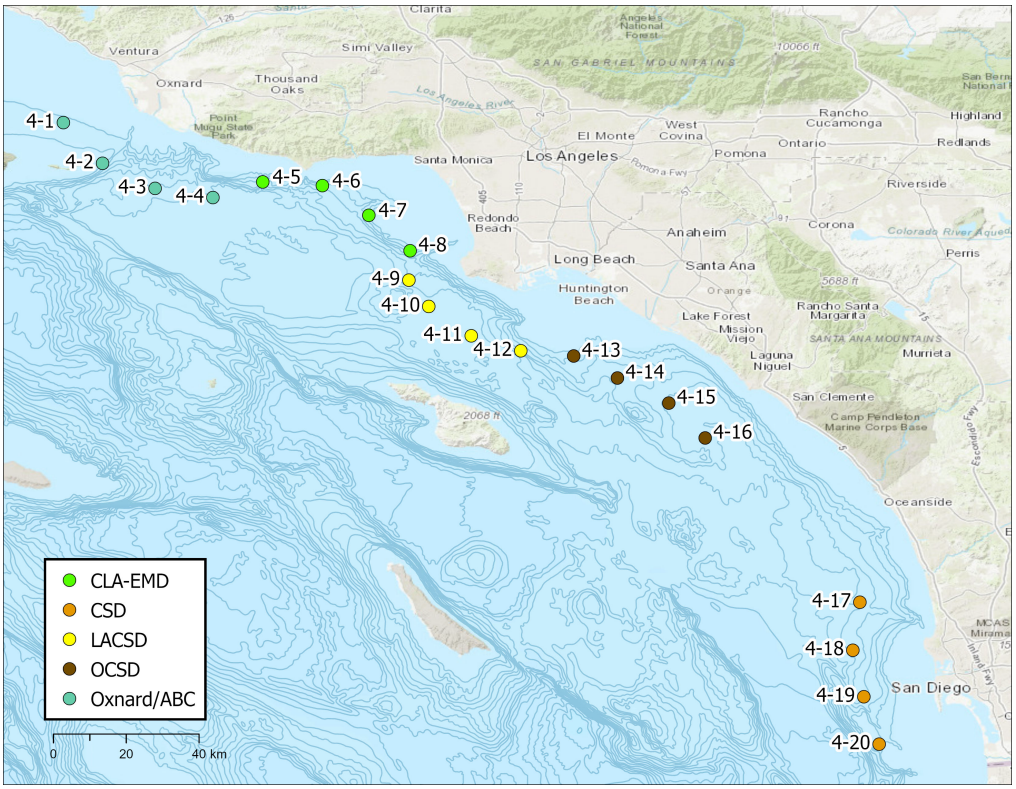

Fig 1. Study Region. Map of sampling sites in the Southern California Bight labeled by station number (4-#) and colored by agency. Dark blue lines represent bathymetry. See S1 Table for for latitude/longitude information and other details.

taxa throughout the upper water column, target depths were treated as approximate rather than exact horizons. After each tow, while the net was still suspended, the mesh was rinsed with filtered seawater to wash material into the cod ends before removal. Cod-end contents were then decanted into a plastic pitcher, briefly allowed to settle, concentrated, and transferred to 250 mL wide-mouth HDPE jars. One cod end was preserved in Zymo DNA/RNA Shield [29] to maintain DNA integrity for molecular analyses, and the other in 190-proof ethanol for a companion shell-dissolution study (not presented here); DNA samples were stored at -20°C until extraction.

Carbonate chemistry characterization

To characterize water-column carbonate chemistry from CTD casts, we relied on empirical linear regressions trained on a water chemistry bottle dataset. Discrete water samples were taken near the surface and at the deepest depth of the CTD casts (typically 150 m) using Niskin bottles. Bottles were analyzed for pH and total alkalinity (TA). pH was measured spectrophotometrically following Liu et al. (2011) [30], and TA was quantified by potentiometric titration [31]. TA and pH, along with CTD-measured temperature and salinity, were used to calculate aragonite saturation state using the R package *seacarb* [32]. We then used the bottle data (n = 218) to fit a linear model with CTD-measured oxygen (O_2) and temperature (T) following Alin et al. (2012) to estimate aragonite saturation state from CTD profiles [33].

$$\Omega_{\mathrm{Ar}}^{\mathrm{est}} = \alpha_0 + \alpha_1 (T - T_r) + \alpha_2 (O_2 - O_{2,r}) + \alpha_3 (T - T_r)(O_2 - O_{2,r}), \quad (1)$$

The fitted parameters were $\alpha_0 = 1.178$, $\alpha_1 = 6.165 \times 10^{-2}$, $\alpha_2 = 5.287 \times 10^{-3}$, $\alpha_3 = 5.799 \times 10^{-4}$, $T_r = 10.28$, and $O_{2,r} = 138.46$, and showed strong agreement with observations ($r^2 = 0.96$; RMSE = 0.124). To propagate CTD oxygen measurement uncertainty, Bayesian model fitting was performed using the R package *brms* [34]. We consider uncertainty in CTD oxygen data in CTD-$\Omega_{\mathrm{Ar}}^{\mathrm{est}}$, since data are collected from multiple agencies using the same sensor model (SBE43) but with differing sensor IDs and calibration procedures. Uncertainty in oxygen sensors is estimated to be no more than $\pm 10\,\mu\mathrm{mol\,kg^{-1}}$, determined from the variation in oxygen conditions at an isopycnal of $25.8\,\mathrm{kg\,m^{-3}}$ across all data (± 1 SD). This oxygen uncertainty propagates an estimated uncertainty in $\Omega_{\mathrm{Ar}}^{\mathrm{est}}$ of ± 0.12 (S1 Fig). See S2 Fig for depth profiles of $\Omega_{\mathrm{Ar}}^{\mathrm{est}}$ compared to the bottle data by station/agency and season, including modeled error in $\Omega_{\mathrm{Ar}}^{\mathrm{est}}$. For comparison with vertically-integrated tow data we average Ω_{Ar} in the upper 15-100 m of the water column, excluding surface waters from analysis.

DNA extraction and sequencing

We homogenized a 50-ml subsample from each Zymo-preserved Bongo net sample in a sterile blender. A 0.8-ml portion was then subjected to bead-beating using the ZymoBIOMICS™ DNA Miniprep D4300 Kit for cell lysis [29]. DNA was extracted from the mesozooplankton samples following the kit manufacturer's protocol to maximize the yield (up to 25 µg of high-quality total DNA [29]) and integrity of the genetic material. Extracted DNA was stored at -80°C until further sequencing. We amplified DNA using the Leray universal metazoan CO1 primer set (mlCOIintF - GGWACWGGWTGAACWGTWTAYCCYCC; mlCOIintR - GGRGGRTASACSGTTCASCCSGTSCC) [35]. Sequencing was performed by Laragen, Inc., using the MiSeq Next-Generation Sequencing using the 2x300 bp chemistry.

Bioinformatics

We processed raw DNA sequence data using REVAMP, an end-to-end sequencing pipeline for amplicon sequencing bioinformatics [36]. REVAMP performs primer and adaptor trimming (Cutadapt v3.7 [37]) before passing reads to DADA2 for length/quality trimming, error correction, dereplication, paired read merging, and generating amplicon sequence variants (ASVs) [38]. ASVs are then taxonomically classified by REVAMP by BLASTing each against all of the nt database (NCBI, downloaded December 2022), filtering to include only the best hits, summarizing the lowest common ancestor of those hits, and cutting off the assigned taxonomy of the ASV at a depth appropriate to the percent identity of the best hit (i.e. high percent identity matches allow for higher confidence in assigning deeper taxonomic ranks; for this run >95% identity for species, 92% genus, 87% family, 77% order, 67% class, 60% phylum, i.e. high percent identities allow for higher confidence in assigning lower taxonomic ranks). To address variable sequencing depths across samples, we converted ASV read counts to relative abundances, enabling robust comparison of community composition across sites and seasons.

Trait-based community classification and correlation to carbonate chemistry

We used Order-level designations to classify all ASVs based on calcification-related traits. Each Order was assigned a calcification status (*yes*, *no*, or *variable*) depending on whether any Families within the Order utilize calcium carbonate minerals in their biochemistry at any point during their life cycle. Orders labeled as *yes* typically use calcium carbonate for structural purposes such as exoskeletons or external shells;

examples include the phyla Mollusca and Echinodermata, both of which are well known for incorporating significant amounts of calcium carbonate into their structures [39]. Orders labeled as *variable* either contain a mix of calcifying and non-calcifying members, incorporate calcium carbonate as a minor component in a composite structure, or differ in calcification status between life stages (e.g., larval vs. adult). For example, certain Orders within the Phylum Arthropoda possess chitinous exoskeletons with only minor calcium carbonate content [40–42]. In addition to calcification status, we assigned each Order a structural type (e.g., exoskeleton, external shell, internal skeleton) and the mineral form associated with that structure (e.g., aragonite, calcite, chitin + calcium). These expanded traits provide a more nuanced understanding of each taxon's potential vulnerability to ocean acidification. To identify novel candidate taxa for use as OA indicators, we analyzed ASV relative abundances across gradients in $\Omega_{\mathrm{Ar}}^{\mathrm{est}}$, incorporating these calcification traits into our bioindicator selection criteria.

Criteria for novel bioindicator candidate selection

We applied four criteria drawn from established bioindicator selection frameworks that emphasize ecological relevance, detectability, mechanistic linkage to stressors, and consistency across space and time [43–47]. (1) Response to OA: we assessed each taxon via (i) correlations between relative abundance and estimated aragonite saturation state ($\Omega_{\mathrm{Ar}}^{\mathrm{est}}$) and (ii) sensitivity documented in the literature, under the assumption that informative indicators show clear, consistent OA–biological relationships and are readily detectable. (2) Abundance and ubiquity: we considered both relative abundance and presence across stations and seasons. Abundant taxa are typically ubiquitous and yield robust correlations with $\Omega_{\mathrm{Ar}}^{\mathrm{est}}$, whereas for low-abundance taxa, widespread occurrence across space and time is more informative. This dual view guides evaluation of both current targets and novel candidates. (3) Phylogenetic coherence: we examined whether closely related ASVs (e.g., within the same Class or Order) showed similar responses to $\Omega_{\mathrm{Ar}}^{\mathrm{est}}$; concordant-level patterns support shared potential sensitivity or tolerance, while discordance warrants cautious interpretation and investigation of ecological or methodological drivers. (4) Calcification traits: assigned at the Order level (structural use and mineral composition), recognizing that taxa building aragonitic or calcitic components may be more susceptible under low Ω_{Ar}. Susceptibility can be life-stage dependent; *variable* Orders may include members or stages with minor calcium carbonate or chitin–calcium composites in their biochemistry. Because many ASVs likely represent larval (meroplanktonic) forms, we interpret correlations in light of trait expression by stage. While microscopy can resolve life-stage structure directly, trait-informed metabarcoding provides a scalable screen; calcification traits add ecological context and help refine candidate selection. Together, these four criteria, applied with attention to ecological and taxonomic nuance, provide a concise, consistent framework for identifying and evaluating candidate bioindicator taxa in the Bight for inclusion in long-term monitoring.

Current targeted versus alternative known resident bioindicator taxa

We examined the biogeographic patterns of two groups of candidate OA bioindicators. First, we assessed the seasonal occurrence of current Bight RMP bioindicator targets: Pteropoda (specifically the species *Limacina helicina*) and *Emerita analoga*. We placed particular emphasis on Pteropoda, a well-established OA indicator Order within the Phylum Mollusca. As a representative decapod species, the Bight RMP selected *Emerita analoga* (Pacific sand crab), given that the Bight lacks populations of Dungeness crab, a commonly used crustacean OA indicator in more northern regions [6, 9, 27]. Second, we

conducted a gap analysis to assess the patterns of a targeted set of epipelagic larval forms of ecologically important benthic invertebrates known to occur in epibenthic trawls in the Bight [48]. From this trawl species list, candidates were first filtered based on the resolution of taxonomic identification in the metabarcoding dataset. Only those taxa with confident species-level assignment were considered, excluding several potential candidates from the trawl database that could not be identified at a high taxonomic resolution in the metabarcodes. From this refined list, we prioritized species based on ubiquity across monitored stations, consistent seasonal occurrence, and known calcifying traits. These criteria led to the selection of three calcifying echinoderms: *Strongylocentrotus purpuratus* (Pacific Purple Sea Urchin), *Ophiopteris papillosa* (Flat-spined Brittle Star), and *Dendraster excentricus* (Eccentric Sand Dollar). We also included two species considered *variable* calcifiers due to their life history or mineral composition: *Hermissenda opalescens*, a gastropod mollusk in the Order Nudibranchia, and *Metacarcinus gracilis* (Graceful Rock Crab), a decapod crustacean.

Data processing and analysis

To explore the relationships between ASV relative abundances and carbonate chemistry, we conducted Spearman correlation analyses using depth-averaged, estimated aragonite saturation state ($\Omega_{\mathrm{Ar}}^{\mathrm{est}}$) from 15–100 meters as a proxy for carbonate chemistry variability. This variable represents the depth range targeted by our zooplankton net tows and captures the full vertical extent of carbonate variability relevant to the organisms sampled. Using an integrated value facilitates consistent ecological interpretation across stations and seasons, aligning chemical conditions with biological sampling depth. Correlations were computed for individual ASVs with at least 50% occurrence across samples. To provide ecological context for interpreting ASV responses, we incorporated trait-based groupings, such as calcification status, structural type, and mineral form, assigned at the Order level. Correlated ASV relative abundances were also organized by taxonomic group to further contextualize patterns of sensitivity or tolerance to changes in carbonate chemistry.

To evaluate whether ASV-$\Omega_{\mathrm{Ar}}^{\mathrm{est}}$ correlation strengths differed among trait-based categorical groupings, we applied a non-parametric statistical workflow appropriate for non-normal data distributions. For each categorical trait variable (e.g., mineral form, calcification status, skeletal structure type), we first used the Kruskal–Wallis rank sum test to assess global differences in Spearman correlation coefficients across groups. When the Kruskal–Wallis test indicated a significant effect, we followed up with pairwise post-hoc comparisons using Dunn's test. Multiple testing correction was applied using the Benjamini–Hochberg method. All analyses were performed in R using the *FSA* [49], *dunn.test* [50], *rcompanion* [51], *multcompView* [52], and *tidyr* [53] packages. Final visualizations were generated using a combination of R, MATLAB, and Krona [54].

Use of generative AI tools

We used ChatGPT (OpenAI), a generative artificial intelligence language model, as a writing and coding assistant during this work. Use was limited to (i) troubleshooting and drafting code snippets for data processing and visualization, and (ii) editing text for clarity, grammar, and concision. ChatGPT was also used to generate preliminary calcification trait assignments for taxa based on author-specified criteria; these preliminary assignments were subsequently reviewed and post-curated by a domain expert, and final trait classifications were determined from expert review and supporting primary sources. The AI tool was not used to generate data, run statistical analyses, or make final scientific decisions. All outputs were checked and validated by the authors.

Results

Seasonal variability in aragonite saturation state

Seasonal comparisons in $\Omega_{\mathrm{Ar}}^{\mathrm{est}}$ revealed a clear progression throughout the year, with the lowest values observed in Spring 2019 and the highest in Fall 2019 (Fig 2). Mean $\Omega_{\mathrm{Ar}}^{\mathrm{est}}$ in Spring 2019 was 1.31 (SD = 0.17), with a minimum of 1.10 and maximum of 1.70, indicating the greatest seasonal variability. In contrast, Fall 2019 had the highest mean value at 1.76 (SD = 0.10), followed closely by Winter 2020 (mean = 1.73, SD = 0.10). Summer 2019 exhibited intermediate values (mean = 1.53, SD = 0.10). The strong seasonal signal in environmental conditions reinforces the importance of considering temporal variability when selecting and interpreting bioindicator taxa.

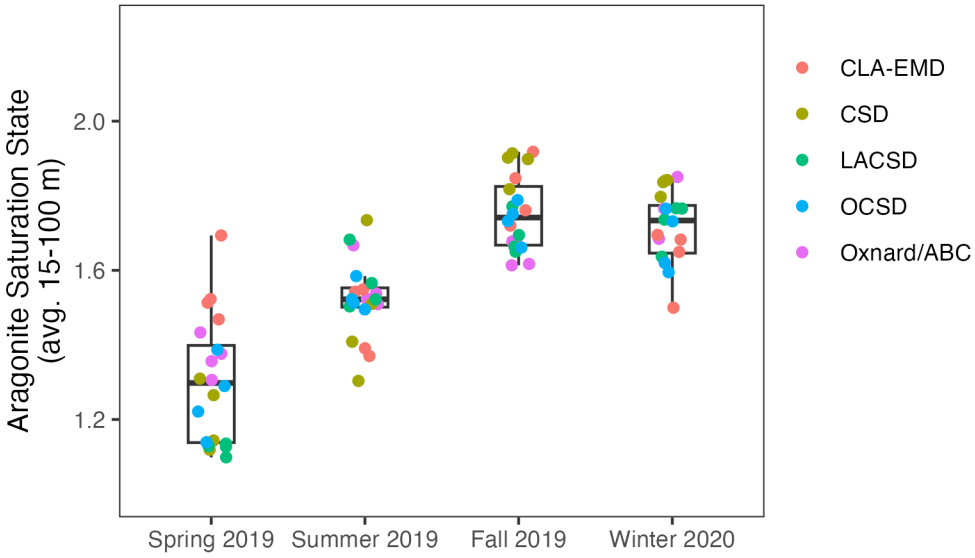

Fig 2. Seasonal Variation in $\Omega_{\mathrm{Ar}}^{\mathrm{est}}$. Boxplots show the distribution of $\Omega_{\mathrm{Ar}}^{\mathrm{est}}$ averaged over the 15–100 m depth range for each season, with colored points indicating individual sampling sites grouped by agency.

Seasonal patterns in mesozooplankton taxonomy

The eighty mesozooplankton samples yielded a mean of 44,108 reads per sample after initial filtering (range: 13,527–87,297), with a mean retention of 79% through trimming/denoising. The final high-quality output averaged 35,000 reads per sample, spanning 12,394–83,565 across samples. Relative-abundance summaries of the top 15 Orders revealed clear seasonal shifts in community composition (Fig 3). These relative abundances reflect sequencing-based compositional signal (i.e., how strongly taxa are represented in the reads) rather than direct estimates of organismal biomass.

Across samples, two Orders dominated the assemblage: Calanoida and Euphausiacea. Calanoida occurred in 100% of samples and had the highest mean relative abundance overall. Within this order, *Calanus pacificus* was the most abundant species, represented by 270 ASVs, present in all samples, and averaging 17.5% relative abundance across samples. Its mean seasonal relative abundance was highest in Summer 2019 (24.7%) and Spring 2019 (23.0%), and lower in Winter 2020 (12.1%) and Fall 2019 (10.2%). *Clausocalanus furcatus* was also prominent, represented by 11 ASVs, present in 82.5% of samples, and averaging 6.0% relative abundance across samples. This species

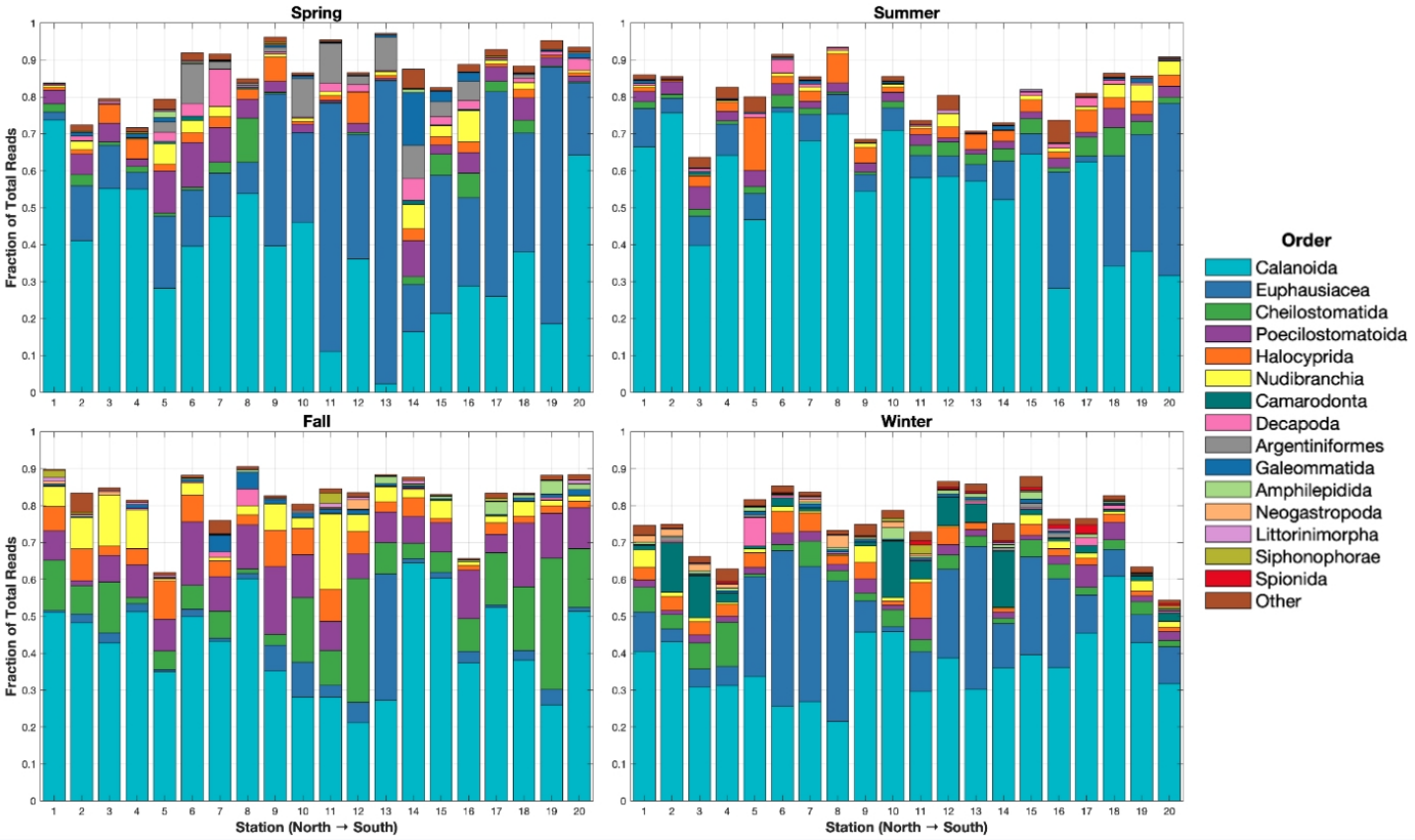

Fig 3. Spatiotemporal Patterns in Mesozooplankton Taxonomy. Proportion of total reads for the 15 most dominant target Orders in read number across sampling sites and seasons with non-target and terrestrial taxa removed. Each bar represents the fraction of the total reads of each taxonomic Order at a given station, with colors denoting different Orders.

showed strong seasonality, with highest mean relative abundance in Fall 2019 (14.6%) and Winter 2020 (8.0%), lower abundance in Summer 2019 (1.38%), and near absence in Spring 2019 (0.005%). Within this species, a single sequence variant (*C. furcatus* ASV 4) was particularly abundant, contributing a mean relative abundance of approximately 3.5% across samples and representing the dominant variant within the species.

Euphausiacea was the second dominant order. Within this group, *Euphausia pacifica* was represented by 36 ASVs, occurred in 98.8% of samples, and averaged 13.5% relative abundance across samples. Its mean seasonal relative abundance was highest in Spring 2019 (25.8%) and Winter 2020 (15.5%), and lower in Summer 2019 (10.1%) and Fall 2019 (2.47%). One sequence variant (*E. pacifica* ASV 1) dominated the krill signal in the dataset and represented the most abundant individual ASV within the community.

Several additional orders contributed consistent secondary components of the whole assemblage. Cheilostomatida, a group of bryozoans represented by 265 ASVs, occurred in all samples and averaged 5.1% relative abundance across samples, with a pronounced seasonal peak in Fall 2019 (11.5%) compared with Spring (2.3%), Summer (2.6%), and Winter (3.9%). Poecilostomatoida, another order of copepods, also occurred in all samples and averaged 5.0% relative abundance across samples. Within this group, *Oncaea scottodicarloi* was the dominant species, represented by 160 ASVs, present in all samples, and averaging 2.4% relative abundance across samples. Its abundance peaked

in Fall 2019 (5.6%) and remained lower but consistent in Spring (1.1%), Summer (1.2%), and Winter (1.8%). Decapoda occurred in 96.3% of samples and averaged 1.0% relative abundance across samples. Within this group, the sandy beach crab *Emerita analoga* was detected only sporadically, represented by 6 ASVs, occurring in 18.8% of samples, and averaging 0.007% relative abundance across samples. Its abundance remained extremely low across seasons, with the highest mean seasonal abundance in Summer 2019 (0.018%). Nudibranchia, an order of gastropod mollusks represented by 253 ASVs, occurred in 95% of samples and averaged 2.4% relative abundance across samples, with a seasonal maximum in Fall 2019 (5.1%).

Littorinimorpha, an order of calcifying gastropod mollusks with shells composed of aragonite and calcite, was represented by 69 ASVs, occurred in 88.8% of samples, and averaged 0.21% relative abundance across samples. Seasonal abundance was highest in Fall 2019 (0.37%) and lower in Winter 2020 (0.18%), Summer 2019 (0.16%), and Spring 2019 (0.12%). Within this order, *Atlanta* (family Atlantidae), a holoplanktonic heteropod gastropod, was the dominant contributing genus, represented by 25 ASVs, present in 81.3% of samples, and averaging 0.15% relative abundance across samples, accounting for approximately 70% of the Littorinimorpha signal. *Atlanta* mirrored the order-level seasonal pattern, with peak abundance in Fall 2019 (0.29%) and lowest mean relative abundance in Winter 2020 (0.075%).

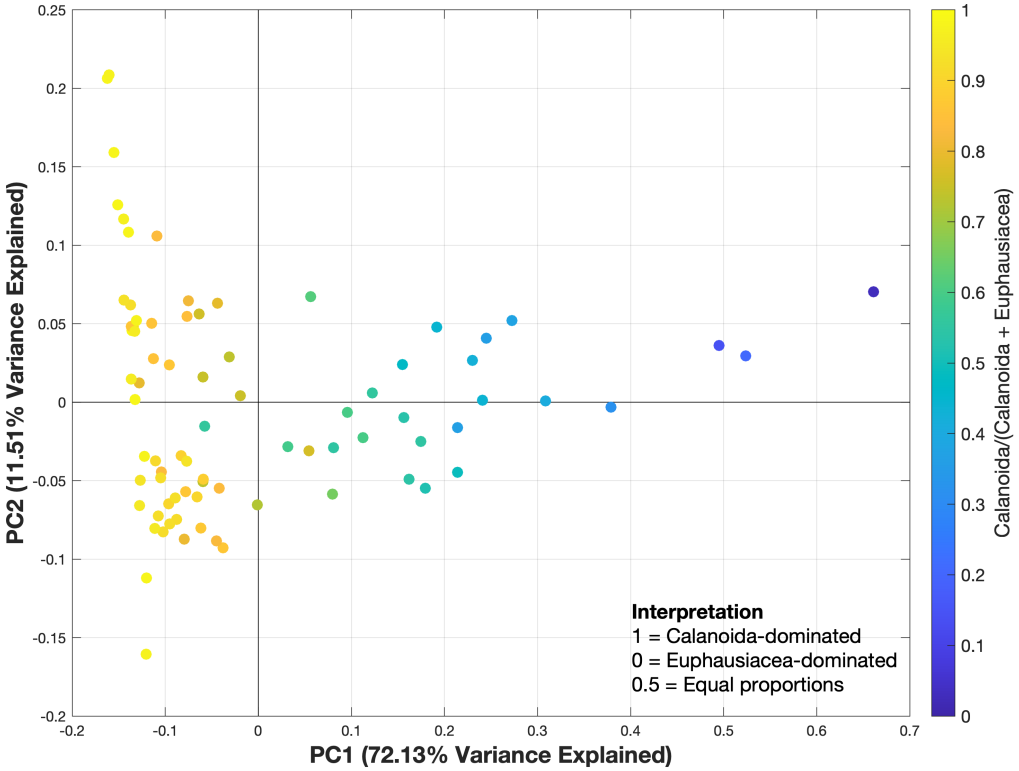

Fig 4. Mesozooplankton Community Drivers. Principal component analysis of the metabarcoding data colored by the ratio of Calanoid copepods to Euphausiid krill, where PC1 explains 72.13% of the variance, and PC2 explains 11.51% of the variance.

Taken together, these patterns indicate that seasonal shifts in the balance between calanoid copepods and euphausiid krill structure much of the observed community turnover across the Southern California Bight. Principal component analysis of ASV relative abundances (Figs 4, S3 Fig) supports this interpretation. PC1 explained 72.1% of the total variance and closely tracked the calanoid-to-euphausiid ratio: samples with

high calanoid dominance clustered at the negative end of PC1, whereas euphausiid-dominated communities clustered at the positive end. This pattern indicates that variation in the balance between Calanoida and Euphausiacea was the primary driver of mesozooplankton community composition across the region.

Trait-based and taxonomic correlates of aragonite saturation state

We evaluated possible bioindicators by correlating the relative abundance of ASVs with estimated aragonite saturation state ($\Omega_{\mathrm{Ar}}^{\mathrm{est}}$), interpreting the sign and magnitude of each coefficient with respect to acidified conditions (low $\Omega_{\mathrm{Ar}}^{\mathrm{est}}$): positive correlations indicate potential sensitivity (declines in relative abundance as $\Omega_{\mathrm{Ar}}^{\mathrm{est}}$ decreases), whereas negative correlations potentially indicate relative tolerance (increases in relative abundance as $\Omega_{\mathrm{Ar}}^{\mathrm{est}}$ decreases). Notably, two individual ASVs emerged as the strongest correlates with $\Omega_{\mathrm{Ar}}^{\mathrm{est}}$ (Fig 5, see S2 Table and S3 Table for more correlation details). An ASV identified as *Calanus pacificus* (calanoid copepod) exhibited the strongest negative correlation ($\mathrm{R}_{\mathrm{Spearman}} = -0.52$, $p < 0.001$, 54% occurrence). An ASV identified as *Clausocalanus furcatus* (calanoid copepod) showed a strong positive correlation with Ω_{Ar} ($\mathrm{R}_{\mathrm{Spearman}} = 0.86$, $p < 0.001$, 80% occurrence). Additional calanoid copepod ASVs showed strong correlations with Ω_{Ar}, following a Genus-level pattern. All positively correlated calanoid ASVs were identified within the genera *Clausocalanus*, *Paracalanus*, or *Candacia*, while all negatively correlated calanoid ASVs were identified as *Calanus pacificus*. Several other ASVs outside the calanoid copepods also exhibited notable correlations with $\Omega_{\mathrm{Ar}}^{\mathrm{est}}$. Euphausiid krill ASVs identified as *Euphausia pacifica* ($\mathrm{R}_{\mathrm{Spearman}} = -0.52$, $p < 0.001$, 99% occurrence) and *Nyctiphanes simplex* ($\mathrm{R}_{\mathrm{Spearman}} = -0.43$, $p < 0.001$, 96% occurrence) showed significant negative correlations. In contrast, an ASV from the Order Halocyprida, identified to the Halocyprididae Family, showed a strong positive correlation ($\mathrm{R}_{\mathrm{Spearman}} = 0.63$, $p < 0.001$, 93% occurrence). Similarly, an ASV from the Order Cheilostomatida, identified to the Membraniporidae Family, also displayed a strong positive correlation ($\mathrm{R}_{\mathrm{Spearman}} = 0.49$, $p < 0.001$, 95% occurrence). Collectively, these results summarize the strongest taxon–$\Omega_{\mathrm{Ar}}^{\mathrm{est}}$ associations observed in the dataset.

Our trait-based analysis (Fig 6) indicate that the relative abundance of ASVs assigned to calcifying taxa, particularly those with aragonite or calcite structures, are more likely to co-vary positively with $\Omega_{\mathrm{Ar}}^{\mathrm{est}}$, supporting their potential utility as bioindicators of acidification conditions in the Bight. ASVs assigned to taxa with confirmed calcium carbonate structures (*yes* calcifiers) exhibited significantly stronger positive correlations with $\Omega_{\mathrm{Ar}}^{\mathrm{est}}$ compared to *variable* or *no* calcifiers (Dunn's test, $p < 0.05$). The median correlations for the non-calcifying and variably calcifying groups were near zero, while the confirmed calcifying group's median correlation was positively shifted. Correspondingly, the ratio of significant positive to significant negative correlations increased with calcification status: *no* calcifiers had a ratio of 0.93, *variable* calcifiers had a ratio of 1.72, and *yes* calcifiers exhibited the highest ratio of 13.5. Mineral form analysis also revealed significant variation in correlation distributions. ASVs with aragonite, aragonite/calcite, or calcite structures showed significantly more positive correlation values compared to chitinous or non-calcifying taxa. *Calcite* and *Aragonite* categories had positive-to-negative ratios of 3.0 and 5.5, respectively, while the *Aragonite/Calcite* group showed only five positive and no negative correlations. In contrast, *Chitin + Calcium* and *None* categories displayed lower ratios of 1.92 and 0.93, respectively. Overall, correlation values with $\Omega_{\mathrm{Ar}}^{\mathrm{est}}$ aligned with expectations among the trait groups summarized in Fig 6.

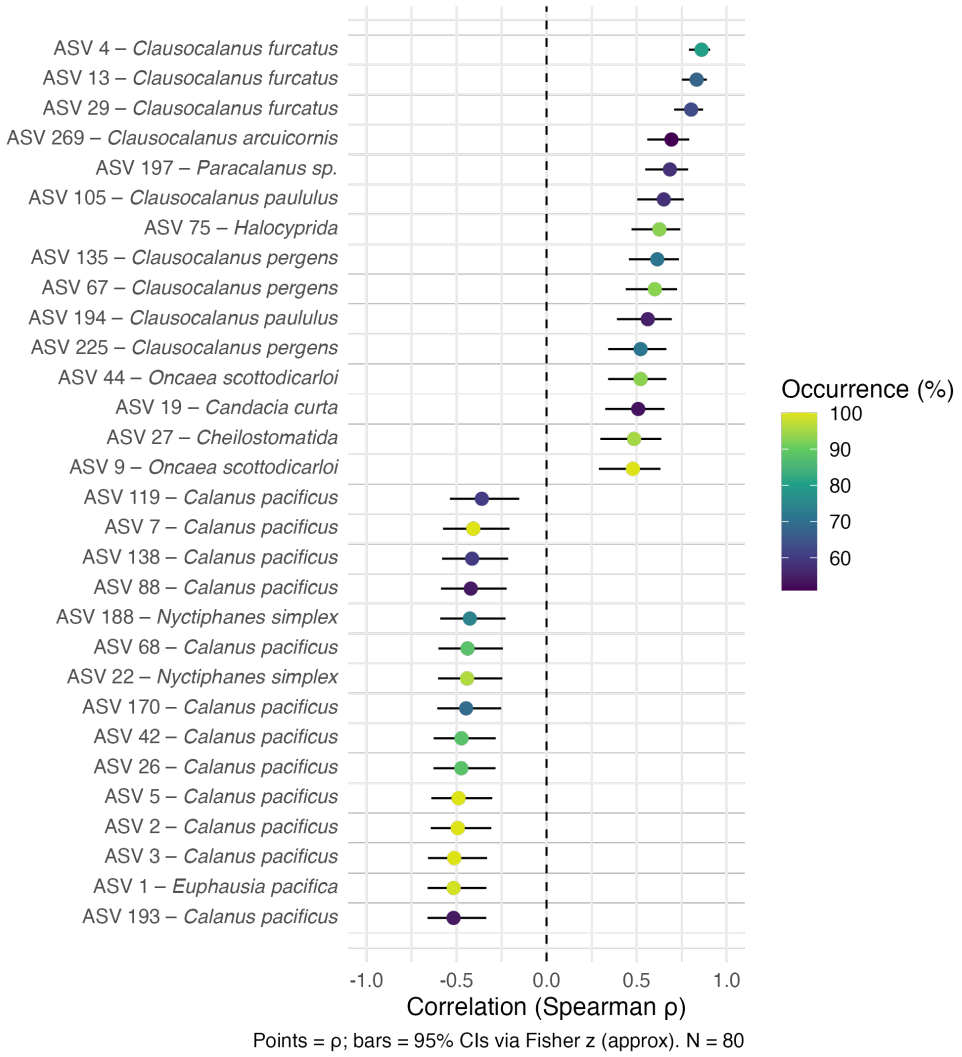

Fig 5. Top 15 Positive & Negative Correlations with $\Omega_{\mathrm{Ar}}^{\mathrm{est}}$. Forest plot of the 30 ASVs with the strongest associations between their relative abundance and $\Omega_{\mathrm{Ar}}^{\mathrm{est}}$. Points show $\mathrm{R}_{\mathrm{Spearman}}$, horizontal lines are 95% confidence intervals computed with the Fisher z transform approximate, and color shows the occurrence percentage (proportion of samples with non-zero relative abundance). Positive values indicate higher relative abundance at higher $\Omega_{\mathrm{Ar}}^{\mathrm{est}}$, whereas negative values indicate higher abundance at lower $\Omega_{\mathrm{Ar}}^{\mathrm{est}}$. All correlations are statistically significant ($\alpha = 0.05$).

Biogeography of currently employed versus candidate resident bioindicator taxa

Seasonal breakdowns in relative abundance across stations for ASVs identified as *E. analoga*, the five benthic invertebrate species (calcifying echinoderms, *Strongylocentrotus purpuratus* (Pacific purple sea urchin), *Ophiopteris papillosa* (flat-spined brittle star), and *Dendraster excentricus* (eccentric sand dollar), gastropod *Hermissenda opalescens* (opalescent nudibranch), an alternative decapod *Metacarcinus gracilis* (graceful rock crab), as well as the three most abundant Families in the Order Pteropoda are visualized in Fig 7.

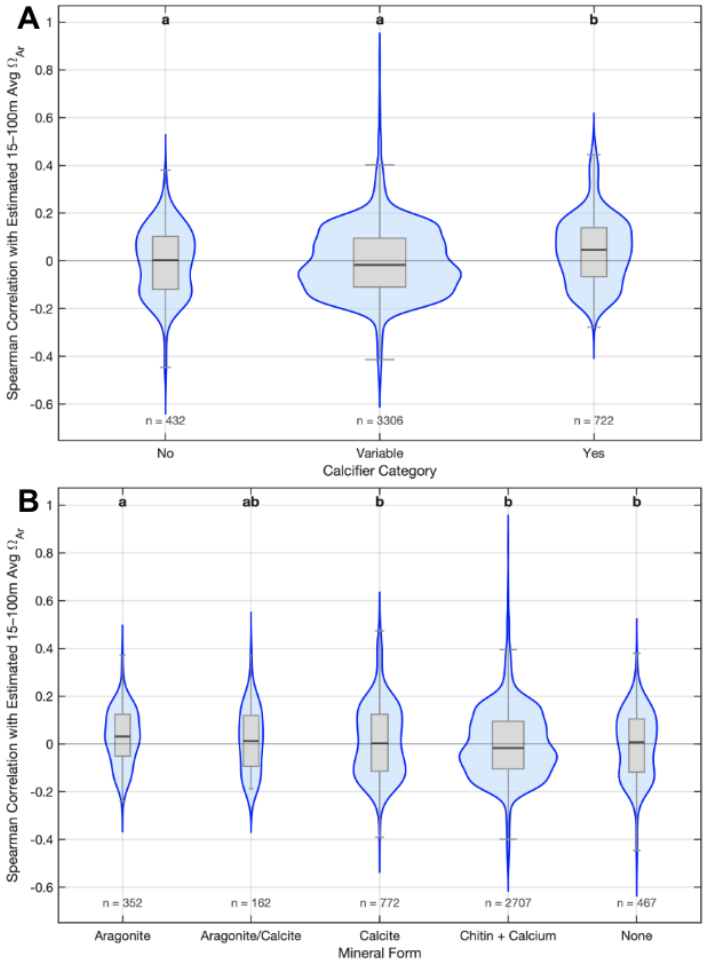

Fig 6. Sensitivity of Calcification Traits to $\Omega_{\mathrm{Ar}}^{\mathrm{est}}$. Correlation coefficients between ASV relative abundance and 15-100-m average $\Omega_{\mathrm{Ar}}^{\mathrm{est}}$ grouped by (A) calcification status and (B) mineral form. Violin plots (light blue) show the kernel density of correlations and are scaled by the number of ASVs per category. Central gray boxplots indicates the median and interquartile range; whiskers extend to 1.5× IQR. Letters above groups denote statistically homogeneous sets from Kruskal–Wallis with Dunn's post-hoc tests (Benjamini–Hochberg FDR, $\alpha = 0.05$); groups sharing a letter are not significantly different.

In our dataset, the Order Pteropoda showed low relative abundance across samples and seasons (Fig 7C), sparse detection at the species level, and limited taxonomic resolution using the CO1 primer (Fig 8). The Order Pteropoda was represented by 111 ASVs, contributing just 0.088% of total reads and appearing in 57 out of 80 samples (71.3% occurrence). Seasonal presence increased across the year, with relative abundances rising from Spring (0.0072% of total reads, 45% occurrence) to Winter (0.0312%, 95%), but overall the relative abundances remained very low. At the species level, only a few pteropods were resolved. *Clio pyramidata* was the most common, with 26 ASVs contributing 0.0101% of total reads and appearing in 32.5% of samples. Seasonally, it was detected in 30–35% of samples per quarter, with relative abundances ranging from from 8×10^{-5} to 2.2×10^{-4} per sample. Other species were detected infrequently: *Creseis conica* appeared in only 11.3% of samples (0.0042% total relative

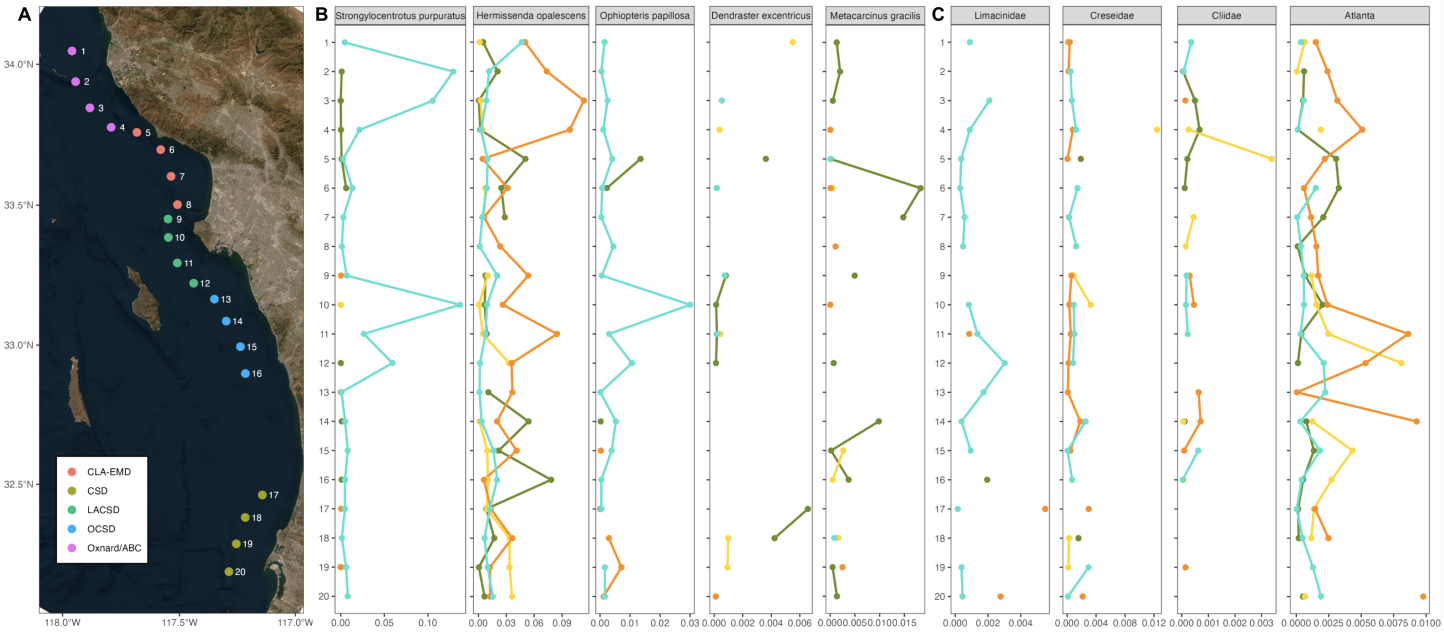

Fig 7. Relative Abundance of Resident Taxa Evaluated as OA Bioindicators. (A) Map of sampling sites color-coded by agency. Relative abundance by season and station of (B) ecologically and management-relevant species that were selected based on ecological importance, potential sensitivity to OA, and prevalence in benthic trawl surveys and (C) holoplanktonic shelled gastropods: the three most abundant Families in the Order Pteropoda (Limacinidae, Creseidae, Cliidae) and the genus *Atlanta* in the Order Littorinimorpha. Note that x-axis scales differ among panels in (B) and (C) to accommodate differences in relative abundance among taxa.

abundance), and *Cuvierina pacifica* and *Creseis virgula* occurred in just 2.5% and 1.3% of samples, respectively. Taxonomic resolution was also limited within the Order. As shown in the Krona [54] visualization, Fig 8, 40% of all Pteropoda reads were assigned only to the Family Cresaeidae with no Genus-level resolution, while an additional 29% belonged to the Family Limacinidae without species-level identification. Only 11% of Pteropoda reads were confidently attributed to *Clio pyramidata*, and less than 5% each to *Cuvierina pacifica*, *Creseis virgula*, and *Creseis conica*. Also shown in Fig 7C, the genus *Atlanta* (Order Littorinimorpha, family Atlantidae) was evaluated alongside pteropods as a holoplanktonic shelled gastropod with aragonite-based shell mineralogy and established sensitivity to ocean acidification. Unlike the Pteropoda, *Atlanta* achieved high species-level resolution: approximately 99% of reads were assigned to *Atlanta* sp. USNM IZ 1230636, and its total read contribution (0.118%) exceeded that of the entire Order Pteropoda (0.088%).

Of the larval stages of epibenthic trawl organisms, *Hermissenda opalescens* was the most relatively abundant and widespread compared to the other four benthic invertebrate species and *E. analoga*, with 178 ASVs contributing 1.55% of total reads and detected in 74 of 80 samples (Fig 7B). The species occurred in all seasons, with the highest seasonal relative abundance in Fall 2019 (0.78%, 100% occurrence), followed by Winter 2020 (0.22%, 100%), Spring 2019 (0.35%, 90%), and Summer 2019 (0.20%, 80%). *Strongylocentrotus purpuratus* was represented by 15 ASVs and contributed 0.56% of total reads. It was detected in 43.75% of samples overall, peaking in Winter 2020 with 0.55% relative abundance and 100% sample occurrence. Spring 2019 showed moderate presence (0.011%, 50%), while Fall 2019 and Summer 2019 showed minimal detection

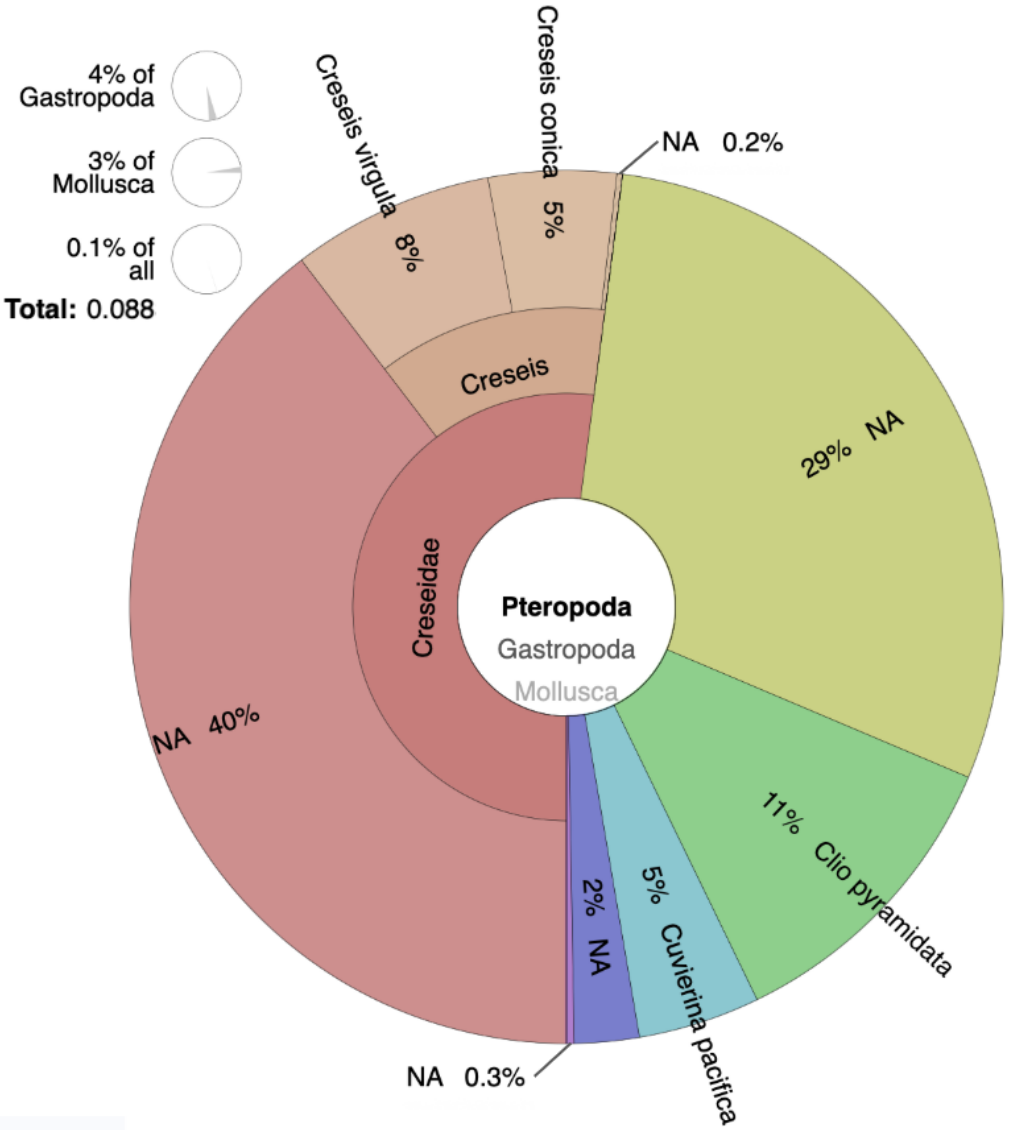

Fig 8. Taxonomic Breakdown of Pteropoda ASVs Based on Read Abundance. Krona [54] visualization showing the hierarchical taxonomic composition of ASVs assigned to the Order Pteropoda. This chart represents a breakdown of only 0.088% of the total read counts in the dataset, reflecting the very low overall relative abundance of pteropods.

(0.0011%, 20%; and 0.00008%, 5%, respectively). *Ophiopteris papillosa* had 14 ASVs contributing 0.10% of total reads, detected in 33.75% of samples overall. Its detection was highest in Winter 2020 (0.073%, 95% occurrence). Lower relative abundances were observed in Fall 2019 (0.012%, 20%) and Spring 2019 (0.016%, 20%), while it was not detected in Summer 2019. *Dendraster excentricus* contributed 0.026% of total reads across 17 samples (21.25%). It showed the greatest relative abundance in Spring 2019 (0.016%, 35% occurrence), with declining detection in Summer 2019 (0.0082%, 25%), Winter 2020 (0.0017%, 20%), and Fall 2019 (0.0001%, 5%). *Metacarcinus gracilis* was represented by 9 ASVs, contributing 0.068% of total reads and present in 30% of samples. Spring 2019 had the highest values (0.058%, 65%), followed by smaller

contributions in Summer (0.0053%, 20%), Fall (0.0037%, 25%), and Winter (0.0009%, 10%). Collectively, these data show that *H. opalescens* exhibited the highest seasonal ubiquity and comparatively greater relative abundance, whereas pteropods and *E. analoga* were uncommon and sparsely resolved taxonomically.

Discussion

Mesozooplankton community diversity and composition

Seasonal variability in mesozooplankton community composition, as revealed through metabarcoding data, was a prominent feature of this study and was also consistent with long-term ecological dynamics documented in the Southern CCE [55–57]. The dominance of Calanoida (copepods) and Euphausiacea (krill) not only dominated community-level relative abundance patterns (Fig 3) but also drove the primary axis of variation (Fig 4), underscoring the ecological significance of these groups for mesozooplankton biogeography. Calanoida were ubiquitous and abundant across all seasons, with a peak in summer that may reflect the seasonal phytoplankton blooms that sustain their populations [58]. Within this Order, species-level responses were seasonally differentiated: *Calanus pacificus* peaked in spring and summer, while *Clausocalanus furcatus* was more dominant in fall and winter [59, 60]. Euphausiids, particularly *Euphausia pacifica*, exhibited classic upwelling-related peaks in winter and spring, aligning with their known associations with La Niña events and enhanced productivity in the California Current [57, 61, 62]. These dynamics highlight the interplay between species-specific phenologies and regional oceanography in shaping seasonal trends in the Bight. The ability of metabarcoding to capture these seasonal shifts strengthens its reliability as a tool for assessing zooplankton community dynamics and environmental responses at finer taxonomic resolutions and reinforces the potential of trait-informed metabarcoding for long-term monitoring of ecosystem responses to environmental variability and climate change.

Identifying novel OA bioindicator candidates

Krill and copepods are among the most abundant and ecologically important zooplankton in the California Current Ecosystem (CCE), including the Southern California Bight [55, 57, 63], and krill have been highlighted by the Ocean Protection Council Science Advisory Team as priority candidates for OA indicator development in regional monitoring programs [64]. Our metabarcoding results (Fig 3, Fig 5) are consistent with this context: copepods (Calanoida, Poecilostomatoida) and krill (Euphausiacea) dominate community variability, and several ASVs within these groups show systematic associations with $\Omega_{\mathrm{Ar}}^{\mathrm{est}}$. The direction of these associations aligns with prior observations and ecology in the CCE. For example, negative correlations of *Calanus pacificus* and Euphausiids with $\Omega_{\mathrm{Ar}}^{\mathrm{est}}$ are compatible with traits that can confer tolerance to low-Ω_{Ar} waters, including frequent exposure to chemical variability via diel vertical migration in *Euphausia pacifica* [65], and with prey-field shifts following upwelling that can differentially favor taxa [66]. Conversely, positive correlations of *Clausocalanus* spp. and *Oncaea scottodicarloi* suggest greater sensitivity to acidified conditions; the latter's abundance has been reported to fluctuate with climate variability [67]. The strong positive signal in the calcifying bryozoan Order Cheilostomatida is consistent with susceptibility of calcium carbonate structures to dissolution [68]), however the stage captured by tows in this study are likely larval and non-calcifying. Taken together, the agreement with prior work strengthens the case that the krill and copepod taxa highlighted by our correlation screening are ecologically

plausible candidates for indicator development in the Bight. At the same time, these associations were identified from a limited spatiotemporal footprint and within a constrained range of estimated carbonate-chemistry conditions, so inferences should be treated as provisional. Moving forward, mechanistic confirmation and multi-stressor validation, ideally using longer time series and broader environmental gradients, will be necessary to determine whether these correlations persist and to establish their reliability for operational monitoring.

The varied responses observed within the copepod Order Calanoida underscore the importance of species-level assessments in indicator development. While members of *Clausocalanus* were positively correlated with $\Omega_{\mathrm{Ar}}^{\mathrm{est}}$, suggesting sensitivity to low Ω_{Ar}, *C. pacificus* exhibited a negative correlation, suggesting tolerance. Similarly, Poecilostomatoida, a closely related copepod Order, also showed overall susceptibility. These co-phylogenetic inconsistencies indicate that Ω_{Ar} responses are not conserved at broad taxonomic levels and reinforce the need for finer-resolution ecological and trait-based interpretation. Species-specific differences in feeding behavior and phytoplankton prey preference, particularly following upwelling events, may help explain these patterns [66]. Thus, ecological traits such as prey selectivity, vertical migration behavior, and life stage-specific calcification likely mediate taxon-specific responses to carbonate chemistry and may vary even among closely related groups. Despite these complexities, the taxa with the strongest correlations are also among the most abundant and ubiquitous in the dataset. Their high frequency of detection supports their statistical reliability and practicality for long-term ecological monitoring. The ability to consistently detect these dominant groups with DNA-based methods enhances their operational viability, particularly when scaled to routine biomonitoring efforts. While these results identify promising bioindicator candidates for the Southern California Bight, they do not establish causation. Continued validation will be necessary to assess the consistency of observed correlations across space, time, and changing ocean conditions. Future efforts should prioritize building longer time series, incorporating concurrent carbonate chemistry measurements, and evaluating physiological mechanisms that drive species-specific responses to OA.

Calcification trait correlation results (Fig 6) provide ecological and mechanistic support for the observed patterns in taxon-specific correlations with $\Omega_{\mathrm{Ar}}^{\mathrm{est}}$. The relative abundance of ASVs assigned to calcifying taxa exhibited significantly more positive correlations with $\Omega_{\mathrm{Ar}}^{\mathrm{est}}$ compared to non-calcifying or variably calcifying groups, reinforcing the hypothesis that biological reliance on calcium carbonate structures increases susceptibility to acidified conditions. Among mineral forms, ASVs associated with aragonite, calcite, or mixed aragonite-calcite structures showed the strongest positive correlation patterns, whereas those with chitinous or non-calcifying biochemistries had lower or neutral associations. This aligns with known differences in mineral solubility; aragonite is more soluble than calcite, making aragonitic organisms particularly vulnerable to undersaturated conditions [69–71]. The known enhanced sensitivity of some larval calcifiers [71] is particularly relevant in this study, as the size-fractionated net tow samples likely captured early life stages, including meroplankton and juveniles. Many taxa labeled as *variable* calcifiers may not express calcium carbonate traits throughout their full life cycle, but do so during vulnerable developmental windows. For example, the nudibranch *Hermissenda opalescens*, categorized in this study as a *variable* calcifier, possesses an aragonitic larval shell during its veliger stage [72], which is sensitive to dissolution under low Ω_{Ar} conditions. These life-stage specific traits help explain why some taxa exhibited positive correlations with $\Omega_{\mathrm{Ar}}^{\mathrm{est}}$ despite being variably or minimally mineralized in adulthood. Thus, structural composition and developmental timing likely influence both the strength and direction of the correlations. While these trait-based patterns lend

credibility to our correlation-based identification of candidate bioindicators, they do not establish causality; rather, they offer a biologically plausible rationale for pursuing targeted validation in long-term monitoring. In this context, metabarcoding provides complementary value beyond shell-dissolution assessments of a few target taxa by resolving community-wide dynamics and revealing how the relative abundances of multiple taxa respond to variability in $\Omega_{\mathrm{AR}}^{\mathrm{est}}$.

Evaluating known targeted versus alternative OA bioindicator candidates

Current target candidates: pteropods & sand crab larvae

Two taxa, pteropods and the decapod *Emerita analoga*, were evaluated for their suitability as the current targeted OA bioindicators in the Bight. Although both have been promoted as leading OA indicators based on extensive work in the Northern CCS and other temperate to arctic regions [9, 28, 65, 73], neither pteropods nor *E. analoga* were ubiquitous across stations in one or more seasons in the Bight and, when present, their abundances were low (Fig 7B & C). This implies that the capture probability and effort required to sort and identify these organisms may render them impractical as routine targets for tracking trends in abundance or shell dissolution.

In our metabarcoding dataset, pteropods were detected at low relative abundance, low ubiquity, and limited taxonomic resolution (Fig 8). Regional context likely contributes to this as the Bight lies near the lower latitudinal edge of many pteropod ranges, potentially constraining their capacity to respond consistently to OA in this region [9]. Methodological factors also likely play a role. Universal markers such as the CO1 primer used here tend to amplify more abundant taxa, potentially reducing detectability of pteropods in mixed assemblages even further. Despite these limitations, including pteropods remains valuable for cross-region comparisons, and future pteropod-focused efforts in the Bight would benefit from more targeted approaches (e.g., improved CO1 primer sets for relative abundance, qPCR for absolute abundance, and updated reference libraries).

Emerita analoga was the second target indicator, selected as a regional decapod proxy in lieu of the Dungeness crab (an established OA indicator in northern CCS) and likewise occurred at low relative abundance and ubiquity. As such, it did not meet the ubiquity necessary for a target in our framework. Decapods in our dataset, including *E. analoga*, were classified as *variable* calcifiers due to their chitinous exoskeletons with embedded calcium carbonate [74]. As such, OA responses among decapods vary considerably by species and life stage. For example, previous work has documented exoskeletal dissolution and mechanoreceptor damage in larval Dungeness crabs (*Metacarcinus magister*) under present-day OA conditions in the northern CCE [9]. Studies have also demonstrated that OA sensitivity in crabs is influenced by environmental stability, with shallow-water species like *M. magister* exhibiting greater physiological tolerance to OA due to frequent exposure to upwelling-driven variability, compared to deep-sea species such as *Chionoecetes tanneri* [75]. These findings underscore the need for further research to evaluate decapod indicators specific to the Bight. Overall, the low and patchy occurrence of both pteropods and *E. analoga*, coupled with uncertain regionality and potential metabarcoding biases, indicates that neither appears suitable for continued OA monitoring in this region.

Emerging resident target candidates

We illustrated how high resolution metabarcoding might be used to identify potential OA bioindicator taxa for continued biological monitoring, drawing from a regional

monitoring program trawl database records [48]. Based on this example of five known candidate organisms (Fig 7B), only *Hermissenda opalescens* (opalescent nudibranch) stands out as the the species that meets the ubiquity and abundance criteria. *Strongylocentrotus purpuratus* (purple sea urchin) was ubiquitous across all stations during winter only, albeit with more limited abundance. In this particular example, because occurrence, abundance and OA sensitivity are likely to vary by the particular species of benthic organism, the lack of taxonomic resolution was a notable impediment to using this approach to identify bioindicator target organisms. Further work is needed to expand the metabarcoding reference libraries to better fully account for possible targets. The question remains whether *H. opalescens* is truly a suitable candidate. Although adult nudibranchs lack extensive mineralized structures, their larval stage possesses an aragonitic calcium carbonate shell [72], making them susceptible to dissolution. Furthermore, *H. opalescens* was highly ubiquitous in our metabarcoding dataset, appearing in 92.5% of samples across all seasons and stations. It also has a known biogeography that extends from the Sea of Cortez in Mexico up to Northern California [76]. This ubiquity, combined with its calcifying larval trait, supports its use as a possible taxon for SEM-based shell condition monitoring and as a broader OA bioindicator candidate. The diel vertical migratory patterns of larval *H. opalescens* is unknown, however, so they may not represent an organism that is exposed to the region of the water column that is rapidly acidifying [2].

The genus *Atlanta* (family Atlantidae) represents another promising resident candidate meriting further consideration. As a permanently holoplanktonic heteropod gastropod bearing a thin aragonitic shell [77], *Atlanta* is directly and continuously exposed to surface water chemistry without the vertical migration uncertainty that complicates interpretation of *H. opalescens* larval signals. Its high occurrence across our dataset (81.3% of samples) indicates consistent regional presence, and its aragonitic mineralogy confers sensitivity to dissolution under reduced carbonate saturation states. Collectively, these traits position *Atlanta* as a candidate well-suited to shell condition monitoring approaches analogous to those applied to pteropods, with the added advantage of substantially better taxonomic resolution in our metabarcoding dataset. More experimental and field studies are needed to evaluate this and other candidate taxa for their utility in long-term OA biomonitoring programs in this dynamic coastal ecosystem.

Conclusions and recommendations

This study represents a contribution in the development of an OA bioindicator program in the Bight, using a metabarcoding approach to evaluate current and novel bioindicator candidate taxa based on their biogeography, ecological relevance, calcification traits, and relationships to $\Omega_{\mathrm{Ar}}^{\mathrm{est}}$. While previous research has identified broadly OA-sensitive taxa such as pteropods and Dungeness crab, the assumption that such indicators are suitable for all regions is not always valid. Our findings highlight that some of these traditional indicators are rare and taxonomically unresolved within the Bight, underscoring the necessity of incorporating regional context into indicator selection. Our results also reinforce the utility of metabarcoding for community-level assessments in dynamic and diverse ecosystems. Metabarcoding effectively captured seasonal shifts in mesozooplankton community composition and dominant taxa, in agreement with established ecological patterns, and revealed how fluctuations in the relative abundance of key taxa, particularly calanoid copepods and euphausiid krill, drove the primary axes of variation across samples. These results demonstrate that molecular-based tools can complement traditional microscopy, especially where larval forms or fragile taxa are challenging to identify.

Average Ω_{Ar}^{est} allowed for expanded spatial coverage in the absence of direct carbonate chemistry sampling and was a useful environmental proxy. Though its derivation from temperature and oxygen data reinforces covariation that complicates mechanistic interpretation, and it should be interpreted as an integrative exposure metric rather than a stand-alone causal driver. Thus, correlation alone does not confirm causality, and all proposed novel bioindicators should be viewed as potential candidates for further evaluation rather than definitive biomarkers. Moreover, the limited spatial and temporal extent of our dataset, combined with methodological constraints in taxonomic resolution, highlights the need for ongoing refinement of reference databases and validation of life stage-specific traits. Looking ahead, regionally tailored indicators identified in this study should be tested in long-term, multi-agency monitoring efforts to assess their operational effectiveness. Metabarcoding holds great promise for enhancing the spatial and temporal resolution of OA monitoring programs and, when used in conjunction with traditional assessment methods, can offer a more comprehensive view of ecosystem change. As OA intensifies alongside other climate stressors, integrating these molecular approaches into routine monitoring frameworks will be essential for preserving marine biodiversity and supporting adaptive management of coastal ecosystems.

Supporting Information

S1 Fig. Observed vs. Predicted Aragonite Saturation State. Relationship between observed and predicted Ω_{Ar} with error bars reflecting uncertainty propagated from the assumed oxygen sensor error. The dashed line indicates the 1:1 reference and the solid red line shows the model fit ($R^2 = 0.96$).

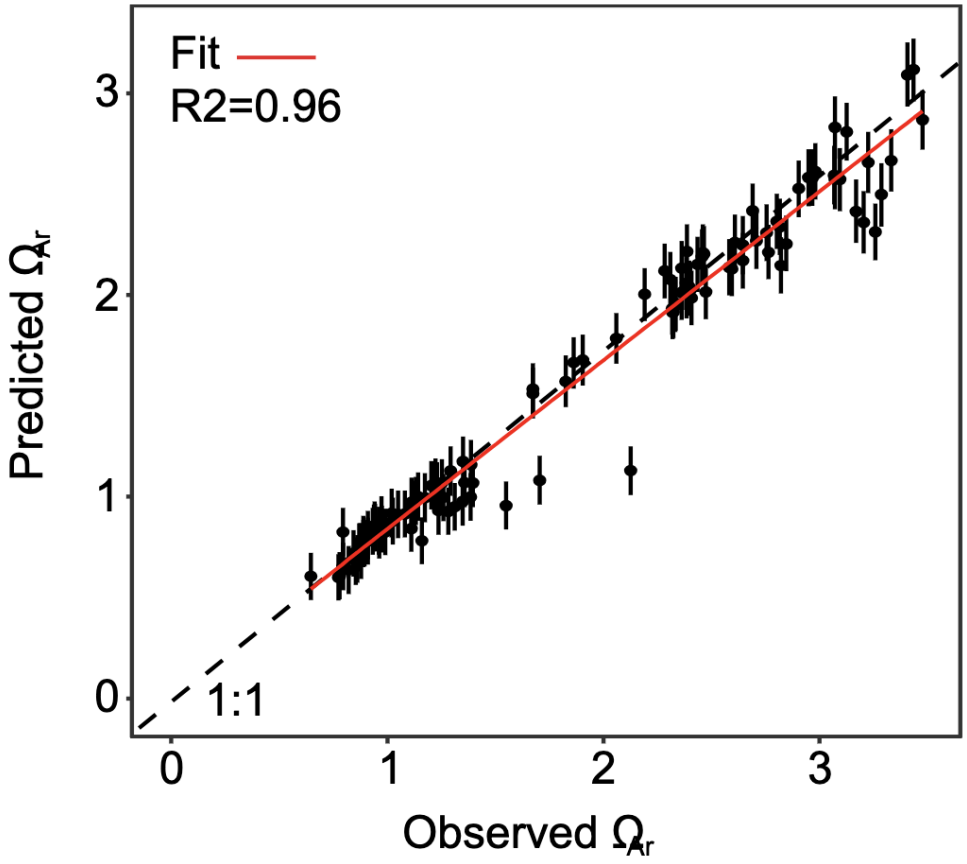

S2 Fig. Ω_{Ar}^{est} by Agency/Station and Season. Depth profiles show Ω_{Ar}^{est} and its estimated error by season at every Agency-Station combination that highlight seasonal aragonite variability within and across stations. Points show bottle data collected as outlined in Methods: Carbonate Chemistry Characterization.

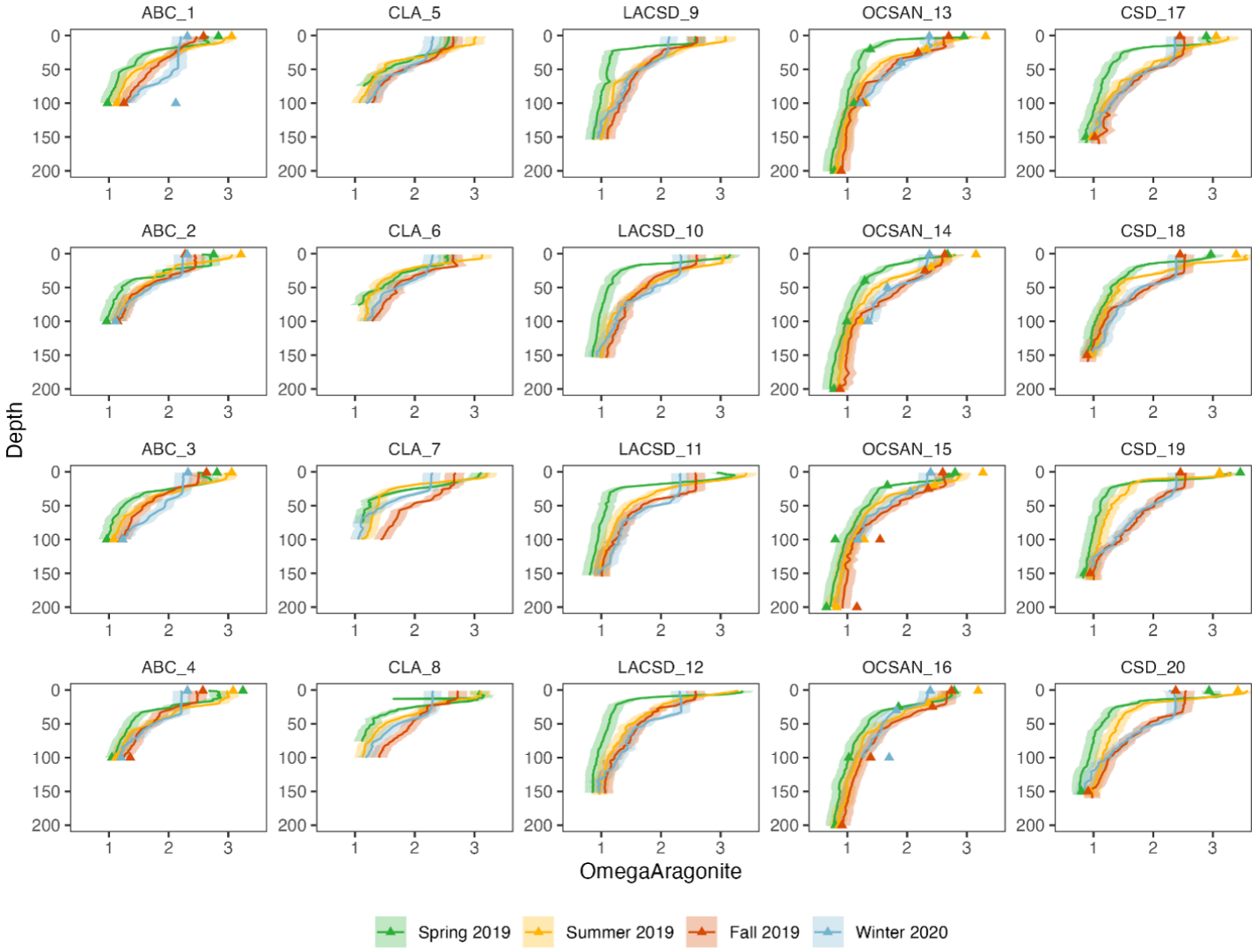

S3 Fig. Mesozooplankton Community by Season. Principal component analysis of the metabarcoding data colored by the sample's season where PC1 explains 72.13% of the variance and PC2 explains 11.51% of the variance.

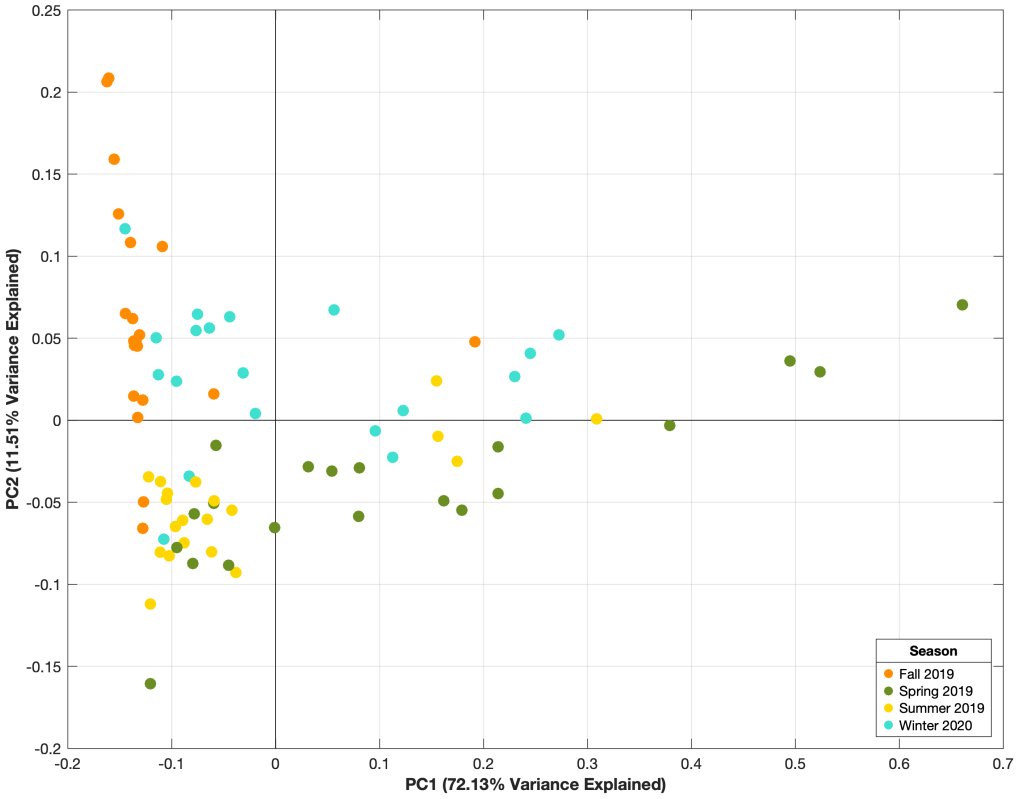

S1 Table. Sampling Dates by Agency, Quarter, and Location. Station labels, their respective agencies, and locations in the Southern California Bight, as well as sampling dates for each quarter per station. CLA-EMD is the City of LA Environmental Monitoring Division; CSD is the Publicly Owned Treatment Works of the City of San Diego; LACSD is the Los Angeles County Sanitation District; OCSD is the Orange County Sanitation District; and Oxnard/ABC is the Publicly Owned Treatment Works of the City of Oxnard. Q1 was Spring 2019, Q2 was Summer 2019, Q3 was Fall 2019, and Q4 was Winter 2020.

Station	Agency	Latitude	Longitude	Q1 Dates	Q2 Dates	Q3 Dates	Q4 Dates
1	Oxnard/ABC	34.120	-119.405	2019-06-23	2019-08-25	2019-11-22	2020-02-07
2	Oxnard/ABC	34.019	-119.308	2019-06-23	2019-08-25	2019-11-22	2020-02-07
3	Oxnard/ABC	33.958	-119.178	2019-06-23	2019-08-25	2019-11-21	2020-02-06
4	Oxnard/ABC	33.935	-119.036	2019-06-23	2019-08-25	2019-11-21	2020-02-06
5	CLA-EMD	33.974	-118.913	2019-05-14	2019-08-13	2019-11-13	2020-02-13
6	CLA-EMD	33.964	-118.765	2019-05-14	2019-08-13	2019-11-13	2020-02-13
7	CLA-EMD	33.891	-118.651	2019-06-11	2019-08-14	2019-11-12	2020-02-11
8	CLA-EMD	33.804	-118.549	2019-06-11	2019-08-20	2019-11-12	2020-02-11
9	LACSD	33.732	-118.552	2019-05-31	2019-08-28	2019-11-25	2020-02-06
10	LACSD	33.667	-118.503	2019-05-31	2019-08-28	2019-11-25	2020-02-06
11	LACSD	33.594	-118.398	2019-05-30	2019-08-29	2019-11-26	2020-02-07
12	LACSD	33.557	-118.276	2019-05-30	2019-08-29	2019-11-26	2020-02-07
13	OCSD	33.544	-118.145	2019-05-14	2019-08-27	2019-11-14	2020-02-20
14	OCSD	33.490	-118.038	2019-05-14	2019-08-26	2019-11-14	2020-02-20
15	OCSD	33.428	-117.911	2019-05-15	2019-08-26	2019-11-13	2020-02-19
16	OCSD	33.342	-117.821	2019-05-15	2019-08-28	2019-11-13	2020-02-19
17	CSD	32.937	-117.440	2019-05-31	2019-08-20	2019-12-05	2020-02-24
18	CSD	32.819	-117.457	2019-05-31	2019-08-20	2019-12-05	2020-02-24
19	CSD	32.704	-117.429	2019-05-31	2019-08-21	2019-12-06	2020-02-28
20	CSD	32.587	-117.392	2019-05-31	2019-08-21	2019-12-06	2020-02-28

S2 Table. Top 15 ASVs with Positive Correlation to Aragonite Saturation (Ω_{Ar}) and High Occurrence. Table includes the top 15 ASVs with occurrence greater than 50% and significant positive correlation to estimated (Ω_{Ar}), as well as calcification traits and a general description derived from the literature and assigned at the Order level.

ASV	Phylum	Class	Order	Family	Genus	Species
4	Arthropoda	Hexanauplia	Calanoida	Clausocalanidae	Clausocalanus	*C. furcatus*
13	Arthropoda	Hexanauplia	Calanoida	Clausocalanidae	Clausocalanus	*C. furcatus*
29	Arthropoda	Hexanauplia	Calanoida	Clausocalanidae	Clausocalanus	*C. furcatus*
269	Arthropoda	Hexanauplia	Calanoida	Clausocalanidae	Clausocalanus	*C. arcuicornis*
197	Arthropoda	Hexanauplia	Calanoida	Paracalanidae	Paracalanus	NA
105	Arthropoda	Hexanauplia	Calanoida	Clausocalanidae	Clausocalanus	*C. paululus*
75	Arthropoda	Ostracoda	Halocyprida	Halocyprididae	NA	NA
135	Arthropoda	Hexanauplia	Calanoida	Clausocalanidae	Clausocalanus	*C. pergens*
67	Arthropoda	Hexanauplia	Calanoida	Clausocalanidae	Clausocalanus	*C. pergens*
194	Arthropoda	Hexanauplia	Calanoida	Clausocalanidae	Clausocalanus	*C. paululus*
225	Arthropoda	Hexanauplia	Calanoida	Clausocalanidae	Clausocalanus	*C. pergens*
44	Arthropoda	Hexanauplia	Poecilostomatoida	Oncaeidae	Oncaea	*O. scottodicarloi*
19	Arthropoda	Hexanauplia	Calanoida	Candaciidae	Candacia	*C. curta*
27	Bryozoa	Gymnolaemata	Cheilostomatida	Membraniporidae	NA	NA
9	Arthropoda	Hexanauplia	Poecilostomatoida	Oncaeidae	Oncaea	*O. scottodicarloi*

ASV	Ω_{Ar} Corr.	p-Value	Occ. (%)	Calcifier	Mineral Form	Description
4	0.86103	0.00000	80	Variable	Chitin + Calcium	Copepods
13	0.83372	0.00000	68	Variable	Chitin + Calcium	Copepods
29	0.80329	0.00000	63	Variable	Chitin + Calcium	Copepods
269	0.69372	0.00000	51	Variable	Chitin + Calcium	Copepods
197	0.68534	0.00000	58	Variable	Chitin + Calcium	Copepods
105	0.65141	0.00000	58	Variable	Chitin + Calcium	Copepods
75	0.62676	0.00000	93	Variable	Chitin + Calcium	Ostracods
135	0.61515	0.00000	71	Variable	Chitin + Calcium	Copepods
67	0.60132	0.00000	93	Variable	Chitin + Calcium	Copepods
194	0.56241	0.00000	55	Variable	Chitin + Calcium	Copepods
225	0.52246	0.00000	71	Variable	Chitin + Calcium	Copepods
44	0.52227	0.00000	93	Variable	Chitin + Calcium	Copepods
19	0.50922	0.00000	53	Variable	Chitin + Calcium	Copepods
27	0.48648	0.00000	95	Yes	Calcite	Encrusting bryozoans
9	0.47989	0.00001	100	Variable	Chitin + Calcium	Copepods

S3 Table. Top 15 ASVs with Negative Correlation to Aragonite Saturation (Ω_{Ar}) and High Occurrence. Table includes the top 15 ASVs with occurrence greater than 50% and significant negative correlation to estimated (Ω_{Ar}), as well as calcification traits and a general description derived from the literature and assigned at the Order level.

ASV	Phylum	Class	Order	Family	Genus	Species
193	Arthropoda	Hexanauplia	Calanoida	Calanidae	Calanus	*C. pacificus*
1	Arthropoda	Malacostraca	Euphausiacea	Euphausiidae	Euphausia	*E. pacifica*
3	Arthropoda	Hexanauplia	Calanoida	Calanidae	Calanus	*C. pacificus*
2	Arthropoda	Hexanauplia	Calanoida	Calanidae	Calanus	*C. pacificus*
5	Arthropoda	Hexanauplia	Calanoida	Calanidae	Calanus	*C. pacificus*
26	Arthropoda	Hexanauplia	Calanoida	Calanidae	Calanus	*C. pacificus*
42	Arthropoda	Hexanauplia	Calanoida	Calanidae	Calanus	*C. pacificus*
170	Arthropoda	Hexanauplia	Calanoida	Calanidae	Calanus	*C. pacificus*
22	Arthropoda	Malacostraca	Euphausiacea	Euphausiidae	Nyctiphanes	*N. simplex*
68	Arthropoda	Hexanauplia	Calanoida	Calanidae	Calanus	*C. pacificus*
188	Arthropoda	Malacostraca	Euphausiacea	Euphausiidae	Nyctiphanes	*N. simplex*
88	Arthropoda	Hexanauplia	Calanoida	Calanidae	Calanus	*C. pacificus*
138	Arthropoda	Hexanauplia	Calanoida	Calanidae	Calanus	*C. pacificus*
7	Arthropoda	Hexanauplia	Calanoida	Calanidae	Calanus	*C. pacificus*
119	Arthropoda	Hexanauplia	Calanoida	Calanidae	Calanus	*C. pacificus*

ASV	Ω_{Ar} Corr.	p-Value	Occ. (%)	Calcifier	Mineral Form	Description
193	-0.51630	0.00000	54	Variable	Chitin + Calcium	Copepods
1	-0.51575	0.00000	99	Variable	Chitin + Calcium	Krill
3	-0.51254	0.00000	100	Variable	Chitin + Calcium	Copepods
2	-0.49318	0.00000	100	Variable	Chitin + Calcium	Copepods
5	-0.48861	0.00001	100	Variable	Chitin + Calcium	Copepods
26	-0.47338	0.00001	88	Variable	Chitin + Calcium	Copepods
42	-0.47237	0.00001	88	Variable	Chitin + Calcium	Copepods
170	-0.44657	0.00003	69	Variable	Chitin + Calcium	Copepods
22	-0.44110	0.00004	96	Variable	Chitin + Calcium	Krill
68	-0.43854	0.00005	88	Variable	Chitin + Calcium	Copepods
188	-0.42582	0.00008	74	Variable	Chitin + Calcium	Krill
88	-0.42063	0.00010	54	Variable	Chitin + Calcium	Copepods
138	-0.41336	0.00014	60	Variable	Chitin + Calcium	Copepods
7	-0.40673	0.00021	100	Variable	Chitin + Calcium	Copepods
119	-0.35929	0.00106	60	Variable	Chitin + Calcium	Copepods

Author contributions

Conceptualization: Karen McLaughlin, Katherine Mackey, Susanna Theroux, Christina A. Frieder, Martha Sutula. **Formal analysis:** Ashton Bandy. **Investigation:** Ashton Bandy. **Methodology:** Ashton Bandy, Adam Martiny, Susanna Theroux, Sean M. McAllister, Zachary Gold, Katherine Mackey, Melissa Brock, Nataly Pineda. **Resources:** Susanna Theroux, Karen McLaughlin, Martha Sutula, Sean M. McAllister, Zachary Gold, Ashton Bandy. **Software:** Ashton Bandy. **Supervision:** Adam Martiny, Susanna Theroux, Martha Sutula, Katherine Mackey. **Validation:** Ashton Bandy, Adam Martiny, Susanna Theroux, Martha Sutula, Christina A. Frieder. **Visualization:** Ashton Bandy. **Writing – original draft:** Ashton Bandy. **Writing – review & editing:** Ashton Bandy, Susanna Theroux, Martha Sutula, Adam Martiny.

People and grants

Funding for the project was provided by the Southern California Coastal Water Research Project Bight '18 Regional Monitoring Program, the Ocean Protection Council (OPC) Grant #C0831023, Ridge to Reef NSF Research Traineeship (award DGE-1735040), Cooperative Institute for Climate, Ocean, & Ecosystem Studies (CICOES) under NOAA Cooperative Agreement NA20OAR4320271 and NA25OARX432C0012 (Contribution No. 2026-1536); Zachary Gold and Sean McAllister were supported by NOAA's Pacific Marine Environmental Laboratory and the NOAA Omics Program.

Data availability

All data underlying the findings of this study are being prepared for submission to the FAIRe data repository and will be made publicly available without restriction before publication. The repository accession information, including a permanent link or DOI, will be added to the manuscript once available. An interactive Krona [54] plot of the mesozooplankton taxonomy is hosted here: https://ashtobashto.github.io/BightRMP-Metabarcoding-Data-2018/KronaPlot.html.

References

1. Feely RA, Sabine CL, Lee K, Berelson W, Kleypas J, Fabry VJ, et al. Impact of Anthropogenic CO2 on the CaCO3 System in the Oceans. Science. 2004;305(5682):362–366. doi:10.1126/science.1097329.

2. Doney SC, Fabry VJ, Feely RA, Kleypas JA. Ocean Acidification: The Other CO2 Problem. Annual Review of Marine Science. 2009;1(1):169–192. doi:10.1146/annurev.marine.010908.163834.

3. Bausch AR, Gallego MA, Harianto J, Thibodeau P, Bednaršek N, Havenhand JN, et al. Influence of Bacteria on Shell Dissolution in Dead Gastropod Larvae and Adult Limacina Helicina Pteropods under Ocean Acidification Conditions. Marine Biology. 2018;165(2):40. doi:10.1007/s00227-018-3293-3.

4. Bednaršek N, Feely RA, Beck MW, Glippa O, Kanerva M, Engström-Öst J. El Niño-Related Thermal Stress Coupled With Upwelling-Related Ocean Acidification Negatively Impacts Cellular to Population-Level Responses in Pteropods Along the California Current System With Implications for Increased Bioenergetic Costs. Frontiers in Marine Science. 2018;5:486. doi:10.3389/fmars.2018.00486.

5. Davis CV, Rivest EB, Hill TM, Gaylord B, Russell AD, Sanford E. Ocean Acidification Compromises a Planktic Calcifier with Implications for Global Carbon Cycling. Scientific Reports. 2017;7(1):2225. doi:10.1038/s41598-017-01530-9.

6. Bednaršek N, Klinger T, Harvey CJ, Weisberg S, McCabe RM, Feely RA, et al. New Ocean, New Needs: Application of Pteropod Shell Dissolution as a Biological Indicator for Marine Resource Management. Ecological Indicators. 2017;76:240–244. doi:10.1016/j.ecolind.2017.01.025.

7. Bednaršek N, Feely RA, Howes EL, Hunt BPV, Kessouri F, León P, et al. Systematic Review and Meta-Analysis Toward Synthesis of Thresholds of Ocean

Acidification Impacts on Calcifying Pteropods and Interactions With Warming. Frontiers in Marine Science. 2019;6:227. doi:10.3389/fmars.2019.00227.

8. Bednaršek N, Carter BR, McCabe RM, Feely RA, Howard E, Chavez FP, et al. Pelagic Calcifiers Face Increased Mortality and Habitat Loss with Warming and Ocean Acidification. Ecological Applications. 2022;32(7). doi:10.1002/eap.2674.

9. Bednaršek N, Feely RA, Beck MW, Alin SR, Siedlecki SA, Calosi P, et al. Exoskeleton Dissolution with Mechanoreceptor Damage in Larval Dungeness Crab Related to Severity of Present-Day Ocean Acidification Vertical Gradients. Science of The Total Environment. 2020;716:136610. doi:10.1016/j.scitotenv.2020.136610.

10. Chan KYK, Sewell MA, Byrne M. Revisiting the larval dispersal black box in the Anthropocene. ICES Journal of Marine Science. 2018;75(6):1841–1848. doi:10.1093/icesjms/fsy097.

11. Theroux S, Sepulveda A, Abbott CL, Gold Z, Watts AW, Hunter ME, et al. What is eDNA method standardisation and why do we need it? Metabarcoding and Metagenomics. 2025;9:e132076. doi:10.3897/mbmg.9.132076.

12. Gallego R, Jacobs-Palmer E, Cribari K, Kelly RP. Environmental DNA Metabarcoding Reveals Winners and Losers of Global Change in Coastal Waters. Royal Society Publishing Proceedings B. 2020;.

13. Song J, Liang D. Community Structure of Zooplankton and Its Response to Aquatic Environmental Changes Based on eDNA Metabarcoding. Journal of Hydrology. 2023;622:129692. doi:10.1016/j.jhydrol.2023.129692.

14. Zhang Z, Bao Y, Fang X, Ruan Y, Rong Y, Yang G. A Circumpolar Study of Surface Zooplankton Biodiversity of the Southern Ocean Based on eDNA Metabarcoding. Environmental Research. 2024;255:119183. doi:10.1016/j.envres.2024.119183.

15. Lacoursière-Roussel A, Howland K, Normandeau E, Grey EK, Archambault P, Deiner K, et al. eDNA Metabarcoding as a New Surveillance Approach for Coastal Arctic Biodiversity. Ecology and Evolution. 2018;8(16):7763–7777. doi:10.1002/ece3.4213.

16. Bellardini D, Russo L, Di Tuccio V, De Luca D, Del Gaizo G, Zampicinini G, et al. Spatiotemporal Changes of Pelagic Food Webs Investigated by Environmental DNA Metabarcoding and Connectivity Analysis. Philosophical Transactions of the Royal Society B: Biological Sciences. 2024;379(1909):20230178. doi:10.1098/rstb.2023.0178.

17. Fernandez S, Ardura A, Martinez JL, Rick J, Machado-Schiaffino G, Garcia-Vazquez E. Plankton Assessment across the Distribution of West African Hake and Tuna Based on eDNA Metabarcoding. Marine Environmental Research. 2024;194:106312. doi:10.1016/j.marenvres.2023.106312.

18. Closek CJ, Santora JA, Starks HA, Schroeder ID, Andruszkiewicz EA, Sakuma KM, et al. Marine Vertebrate Biodiversity and Distribution Within the Central California Current Using Environmental DNA (eDNA) Metabarcoding and Ecosystem Surveys. Frontiers in Marine Science. 2019;6:732. doi:10.3389/fmars.2019.00732.

19. Pitz KJ, Guo J, Johnson SB, Campbell TL, Zhang H, Vrijenhoek RC, et al. Zooplankton Biogeographic Boundaries in the California Current System as Determined from Metabarcoding. PLOS ONE. 2020;15(6):e0235159. doi:10.1371/journal.pone.0235159.

20. Osborne EB, Thunell RC, Gruber N, Feely RA, Benitez-Nelson CR. Decadal variability in twentieth-century ocean acidification in the California Current Ecosystem. Nature Geoscience. 2020;13(1):43–49. doi:10.1038/s41561-019-0499-z.

21. Dong C, Idica EY, McWilliams JC. Circulation and Multiple-Scale Variability in the Southern California Bight. Progress in Oceanography. 2009;82(3):168–190. doi:10.1016/j.pocean.2009.07.005.

22. Feely RA, Sabine CL, Hernandez-Ayon JM, Ianson D, Hales B. Evidence for Upwelling of Corrosive "Acidified" Water onto the Continental Shelf. Science. 2008;320(5882):1490–1492. doi:10.1126/science.1155676.

23. Gruber N, Hauri C, Lachkar Z, Loher D, Frölicher TL, Plattner GK. Rapid Progression of Ocean Acidification in the California Current System. Science. 2012;337(6091):220–223. doi:10.1126/science.1216773.

24. McLaughlin K, Nezlin NP, Weisberg SB, Dickson AG, Booth JAT, Cash CL, et al. Seasonal Patterns in Aragonite Saturation State on the Southern California Continental Shelf. Continental Shelf Research. 2018;167:77–86. doi:10.1016/j.csr.2018.07.009.

25. Satterthwaite E, Lampe R, Gold Z, Thompson A, Bowlin N, Swalethorp R, et al. Toward Identifying the Critical Ecological Habitat of Larval Fishes: An Environmental DNA Window into Fisheries Management. Oceanography. 2023;doi:10.5670/oceanog.2023.s1.29.

26. Bednaršek N, Možina J, Vogt M, O'Brien C, Tarling GA. The global distribution of pteropods and their contribution to carbonate and carbon biomass in the modern ocean. Earth System Science Data. 2012;4(1):167–186. doi:10.5194/essd-4-167-2012.

27. Bednaršek N, Feely RA, Tolimieri N, Hermann AJ, Siedlecki SA, Waldbusser GG, et al. Exposure History Determines Pteropod Vulnerability to Ocean Acidification along the US West Coast. Scientific Reports. 2017;7(1):4526. doi:10.1038/s41598-017-03934-z.

28. Niemi A, Bednaršek N, Michel C, Feely RA, Williams W, Azetsu-Scott K, et al. Biological Impact of Ocean Acidification in the Canadian Arctic: Widespread Severe Pteropod Shell Dissolution in Amundsen Gulf. Frontiers in Marine Science. 2021;8:600184. doi:10.3389/fmars.2021.600184.

29. Zymo Research. ZymoBIOMICS™ DNA Miniprep Kit; 2023. Zymo Research Corporation.

30. Liu X, Patsavas MC, Byrne RH. Purification and Characterization of meta-Cresol Purple for Spectrophotometric Seawater pH Measurements. Environmental Science & Technology. 2011;45(11):4862–4868. doi:10.1021/es200665d.

31. Dickson AG, Afghan JD, Anderson GC. Reference materials for oceanic CO2 analysis: a method for the certification of total alkalinity. Marine Chemistry. 2003;80(2-3):185–197. doi:10.1016/S0304-4203(02)00133-0.

32. Gattuso JP, Epitalon JM, Lavigne H, Orr J. seacarb: Seawater Carbonate Chemistry; 2003. Available from: `https://CRAN.R-project.org/package=seacarb`.

33. Alin SR, Feely RA, Dickson AG, Hernández-Ayón JM, Juranek LW, Ohman MD, et al. Robust empirical relationships for estimating the carbonate system in the southern California Current System and application to CalCOFI hydrographic cruise data (2005–2011). Journal of Geophysical Research: Oceans. 2012;117(C5):2011JC007511. doi:10.1029/2011JC007511.

34. Bürkner PC. Bayesian Item Response Modeling in R with brms and Stan. Journal of Statistical Software. 2021;100(5):1–54. doi:10.18637/jss.v100.i05.

35. Leray M, Yang JY, Meyer CP, Mills SC, Agudelo N, Ranwez V, et al. A New Versatile Primer Set Targeting a Short Fragment of the Mitochondrial COI Region for Metabarcoding Metazoan Diversity: Application for Characterizing Coral Reef Fish Gut Contents. Frontiers in Zoology. 2013;10(1):34. doi:10.1186/1742-9994-10-34.

36. McAllister SM, Paight C, Norton EL, Galaska MP. SPOTLIGHT ON REVAMP Rapid Exploration and Visualization Through an Automated Metabarcoding Pipeline. Oceanography. 2023;36(2/3):114–119.

37. Martin M. Cutadapt Removes Adapter Sequences from High-Throughput Sequencing Reads. EMBnetjournal. 2011;v. 17(n. 1):10–12. doi:10.14806/ej.17.1.200.

38. Callahan BJ, McMurdie PJ, Rosen MJ, Han AW, Johnson AJA, Holmes SP. DADA2: High-resolution Sample Inference from Illumina Amplicon Data. Nature Methods. 2016;13(7):581–583. doi:10.1038/nmeth.3869.

39. Ruppert EE, Fox RS, Barnes RD. Invertebrate Zoology: A Functional Evolutionary Approach. 7th ed. Belmont, CA: Thomson-Brooks/Cole; 2004.

40. Zainol Abidin NA, Kormin F, Zainol Abidin NA, Mohamed Anuar NAF, Abu Bakar MF. The Potential of Insects as Alternative Sources of Chitin: An Overview on the Chemical Method of Extraction from Various Sources. International Journal of Molecular Sciences. 2020;21(14):4978. doi:10.3390/ijms21144978.

41. Wærvågen SB, A Rukke N, Hessen DO. Calcium Content of Crustacean Zooplankton and Its Potential Role in Species Distribution. Freshwater Biology. 2002;47(10):1866–1878. doi:10.1046/j.1365-2427.2002.00934.x.

42. Engström-Öst J, Glippa O, Feely RA, Kanerva M, Keister JE, Alin SR, et al. Eco-Physiological Responses of Copepods and Pteropods to Ocean Warming and Acidification. Scientific Reports. 2019;9(1):4748. doi:10.1038/s41598-019-41213-1.

43. Heink U, Kowarik I. What Criteria Should Be Used to Select Biodiversity Indicators? Biodiversity and Conservation. 2010;19(13):3769–3797. doi:10.1007/s10531-010-9926-6.

44. Siddig AAH, Ellison AM, Ochs A, Villar-Leeman C, Lau MK. How Do Ecologists Select and Use Indicator Species to Monitor Ecological Change? Insights from 14 Years of Publication in Ecological Indicators. Ecological Indicators. 2016;60:223–230. doi:10.1016/j.ecolind.2015.06.036.

45. Puig-Gironès R, Real J. A Comprehensive but Practical Methodology for Selecting Biological Indicators for Long-Term Monitoring. PLOS ONE. 2022;17(3):e0265246. doi:10.1371/journal.pone.0265246.

46. Håkanson L, Blenckner T. A Review on Operational Bioindicators for Sustainable Coastal Management—Criteria, Motives and Relationships. Ocean & Coastal Management. 2008;51(1):43–72. doi:10.1016/j.ocecoaman.2007.04.005.

47. Wolfe DA. Selection of Bioindicators of Pollution for Marine Monitoring Programmes. Chemistry and Ecology. 1992;6(1-4):149–167. doi:10.1080/02757549208035269.

48. Wisenbaker K, McLaughlin K, Diehl D, Latker A, Stolzenbach K, Gartman R, et al. Southern California Bight 2018 Regional Marine Monitoring Program: Volume IV. Demersal Fishes and Megabenthic Invertebrates. Costa Mesa, CA: Southern California Coastal Water Research Project; 2021. Technical Report #1183.

49. Ogle DH, Doll JC, Wheeler AP, Dinno A. FSA: Simple Fisheries Stock Assessment Methods; 2015. Available from: `https://CRAN.R-project.org/package=FSA`.

50. Alexis Dinno. dunn.test: Dunn's Test of Multiple Comparisons Using Rank Sums; 2014. Available from: `https://CRAN.R-project.org/package=dunn.test`.

51. Mangiafico S. rcompanion: Functions to Support Extension Education Program Evaluation; 2016. Available from: `https://CRAN.R-project.org/package=rcompanion`.

52. Spencer Graves, Hans-Peter Piepho and Luciano Selzer with help from Sundar Dorai-Raj. multcompView: Visualizations of Paired Comparisons; 2006. Available from: `https://CRAN.R-project.org/package=multcompView`.

53. Wickham H, Averick M, Bryan J, Chang W, McGowan L, François R, et al. Welcome to the Tidyverse. Journal of Open Source Software. 2019;4(43):1686. doi:10.21105/joss.01686.

54. Ondov BD, Bergman NH, Phillippy AM. Interactive Metagenomic Visualization in a Web Browser. BMC Bioinformatics. 2011;12(1). doi:10.1186/1471-2105-12-385.

55. Lavaniegos BE, Ohman MD. Coherence of Long-Term Variations of Zooplankton in Two Sectors of the California Current System. Progress in Oceanography. 2007;75(1):42–69. doi:10.1016/j.pocean.2007.07.002.

56. Brinton E. Population Biology of Euphausia Pacifica Off Southern California. Fishery Bulletin. 1976;74(4).

57. Brinton E, Townsend A. Decadal Variability in Abundances of the Dominant Euphausiid Species in Southern Sectors of the California Current. Deep Sea Research Part II: Topical Studies in Oceanography. 2003;50(14-16):2449–2472. doi:10.1016/S0967-0645(03)00126-7.

58. May-Kú MA, Ornelas-Roa M, Suárez-Morales E. Surface Copepod Assemblages in Shallow Coastal Waters off Northeastern Yucatan Peninsula Influenced by the Yucatan Upwelling. Regional Studies in Marine Science. 2022;56:102718. doi:10.1016/j.rsma.2022.102718.

59. Lavaniegos BE, Jiménez-Pérez LC. Biogeographic Inferences of Shifting Copepod Distribution during 1997-1999 El Niño and La Niña in the California Current. Contributions to the Study of East Pacific Crustaceans. 2006;4(1):113–158.

60. Palomares-García RJ, Gómez-Gutiérrez J, Robinson CJ. Winter and Summer Vertical Distribution of Epipelagic Copepods in the Gulf of California. Journal of Plankton Research. 2013;35(5):1009–1026. doi:10.1093/plankt/fbt052.

61. Lavaniegos BE, Ambriz-Arreola I. Interannual Variability in Krill off Baja California in the Period 1997–2005. Progress in Oceanography. 2012;97–100:164–173. doi:10.1016/j.pocean.2011.11.008.

62. McLaskey AK, Keister JE. An Integrated Field-Laboratory Investigation of the Effects of Low Oxygen and pH on North Pacific Krill (Euphausia Pacifica). Marine Biology. 2021;168(4):43. doi:10.1007/s00227-021-03845-8.

63. Hooff RC, Peterson WT. Copepod Biodiversity as an Indicator of Changes in Ocean and Climate Conditions of the Northern California Current Ecosystem. Limnology and Oceanography. 2006;51(6):2607–2620. doi:10.4319/lo.2006.51.6.2607.

64. Team OPCSA. Establishing Science-based Indicators for California's Oceans and Coasts. California Ocean Protection Council, California Ocean Science Trust. 2024;.

65. Keil KE, Klinger T, Keister JE, McLaskey AK. Comparative Sensitivities of Zooplankton to Ocean Acidification Conditions in Experimental and Natural Settings. Frontiers in Marine Science. 2021;8. doi:10.3389/fmars.2021.613778.

66. Mackey KRM, Morris JJ, Morel F, Kranz S. Response of Photosynthesis to Ocean Acidification. Oceanography. 2015;25(2):74–91. doi:10.5670/oceanog.2015.33.

67. Thompson PA, Bonham P, Thomson P, Rochester W, Doblin MA, Waite AM, et al. Climate Variability Drives Plankton Community Composition Changes: The 2010–2011 El Niño to La Niña Transition around Australia. Journal of Plankton Research. 2015;37(5):966–984. doi:10.1093/plankt/fbv069.

68. Smith AM. Growth and Calcification of Marine Bryozoans in a Changing Ocean. The Biological Bulletin. 2014;226(3):203–210. doi:10.1086/BBLv226n3p203.

69. Kleypas J, Feely R, Langdon C, Fabry VJ, Chris S, Robbins LL. Impacts of Ocean Acidification on Coral Reefs and Other Marine Calcifiers: A Guide for Future Research; 2006.

70. Figuerola B, Hancock AM, Bax N, Cummings VJ, Downey R, Griffiths HJ, et al. A Review and Meta-Analysis of Potential Impacts of Ocean Acidification on Marine Calcifiers From the Southern Ocean. Frontiers in Marine Science. 2021;8:584445. doi:10.3389/fmars.2021.584445.

71. Leung JYS, Zhang S, Connell SD. Is Ocean Acidification Really a Threat to Marine Calcifiers? A Systematic Review and Meta-Analysis of 980+ Studies Spanning Two Decades. Small. 2022;18(35):2107407. doi:10.1002/smll.202107407.

72. Eyster LS. Shell Inorganic Composition and Onset of Shell Mineralization During Bivalve and Gastropod Embryogenesis. The Biological Bulletin. 1986;170(2):211–231. doi:10.2307/1541804.

73. Janssen AW, Bush SL, Bednaršek N. The Shelled Pteropods of the Northeast Pacific Ocean (Mollusca: Heterobranchia, Pteropoda). Zoosymposia. 2019;13(1):305–346. doi:10.11646/zoosymposia.13.1.22.

74. Kroeker KJ, Kordas RL, Crim RN, Singh GG. Meta-analysis Reveals Negative yet Variable Effects of Ocean Acidification on Marine Organisms. Ecology Letters. 2010;13(11):1419–1434. doi:10.1111/j.1461-0248.2010.01518.x.

75. Pane E, Barry J. Extracellular Acidbase Regulation during Short-Term Hypercapnia Is Effective in a Shallow-Water Crab, but Ineffective in a Deep-Sea Crab. Marine Ecology Progress Series. 2007;334:1–9. doi:10.3354/meps334001.

76. Estores-Pacheco ALK. Preliminary Characteristics of Two Pseudocryptic Hermissenda Sea Slug Species [Master of Science in Biological Sciences]. California State Polytechnic University. Pomona, California; 2020.

77. Moreno-Alcántara M, Aceves-Medina G, Lavaniegos BE, Hernández-Ayón JM, Jiménez-Rosenberg SPA, Gómez-Gutiérrez J. Seasonal and interannual variability of Atlantidae heteropods along the west coast of Baja California, Mexico. Progress in Oceanography. 2025;239:103562. doi:https://doi.org/10.1016/j.pocean.2025.103562.